ADVANCED THERAPEUTICS
www.advtherap.com

Bicyclic Boronate β-Lactamase Inhibitors: The Present Hope against Deadly Bacterial Pathogens

*Emilio Lence and Concepción González-Bello**

Dedicated to Prof. Javier Benavente on the occasion of his retirement.

The use of β-lactamase inhibitors in combination with β-lactam antibiotics is an emerging area in drug discovery. This strategy allows the restoration of the therapeutic efficacy of these antibiotics in clinical use against multiresistant bacteria. These pathogens are drug resistant because they express β-lactamase enzymes, which prevent the antibiotic therapeutic action by catalyzing the hydrolysis of the β-lactam ring. These enzymes are quite diverse in both their structural architecture and hydrolytic capability, as well as in the mechanism of action. The ever-increasing emergence of pathogens that are capable of coproducing different types of β-lactamases has triggered the search for ultrabroad-spectrum inhibitors capable of deactivating both serine- and metallo-β-lactamases. A recent breakthrough in this long-pursued and unmet need is the discovery of bicyclic boronate inhibitors, specifically taniborbactam, VNRX-7145, and QPX7728, which are currently under clinical development in combination with cefepime, ceftibuten, and QPX2014, respectively. The present article highlights the therapeutic potential of these inhibitors and their spectrum of efficacy is compared with those of other β-lactam/β-lactamase inhibitor combinations recently approved by the food and drug administration. The molecular basis of the ultrabroad-spectrum of activity of boron-based inhibitors is also discussed, on the basis of the available crystal structures and the results of computational studies.

1. Resistance Breakers: The Right Antibiotic Partner for Reversing Antibiotic Drug Resistance

The ability of antibiotics to cure bacterial infections is nowadays in serious danger due to the emergence and dissemination worldwide of multidrug-resistant bacteria.[1–3] These pathogens have evolved by developing highly sophisticated, and sometimes unpredictable, mechanisms to avoid the action of antibiotics.[4] The increasing impact of these deadly pathogens in healthcare systems is worrisome, since in these cases the compromised immune system of patients facilitates the pathogenicity. Resistance to antibiotics is reaching such dangerous levels that the World Health Organization (WHO) estimates that by 2050 deaths from antibiotic resistance will exceed those caused by cancer, and around ten million people could die every year because of this problem.[5] Despite this alarming estimate, the number of new classes of antibiotics approved in the last 50 years, either by disabling unexploited bacterial targets or with a new mechanism of action, is rather low.[6] Thus, most of the antibacterial drugs in the pipeline involve chemical modifications of earlier discoveries to make them more efficient against resistant bacteria.[7] The limited profit margin of the anti-infective therapies (short-term treatments) hinders the recovery of the huge investment costs required to identify research niches and develop small molecules that target them, and this seems to be the main reason why antibiotic discovery programs have been discontinued by the big pharmaceutical companies. In fact, most of the new compounds in this area are being developed by small biotechnology companies. Another drawback is the policy of minimizing the use of the latest generation antibiotics because it goes against the basic principle of any company, i.e., the need to sell drugs to make money and be profitable. A reimbursement reform is also needed to make pharmaceutical companies more attractive businesses for investors.

A review of the clinical antibacterial drug pipeline reveals that current research efforts are focused on restoring the efficacy of antibiotics in clinical use, which have proven to be safe and effective over the years. This successful and growing area of investigation involves the administration of the antibiotic in combination with a compound that either blocks a certain bacterial resistance mechanism or potentiates the action of the drug by facilitating its permeabilization into the bacterium. These compounds are known as "resistance breakers," "antibiotic adjuvants" or "antibiotic potentiators," and they usually lack relevant bactericidal activity in the dose that is administered.[8–20] Among them, β-lactamase inhibitors are the most prominent as they have proven to be the most successful compounds in restoring the efficacy of

Dr. E. Lence, Prof. C. González-Bello
Centro Singular de Investigación en Química Biolóxica e Materiais Moleculares (CiQUS), Departamento de Química Orgánica
Universidade de Santiago de Compostela
calle Jenaro de la Fuente s/n, Santiago de Compostela 15782, Spain
E-mail: concepcion.gonzalez.bello@usc.es

DOI: 10.1002/adtp.202000246

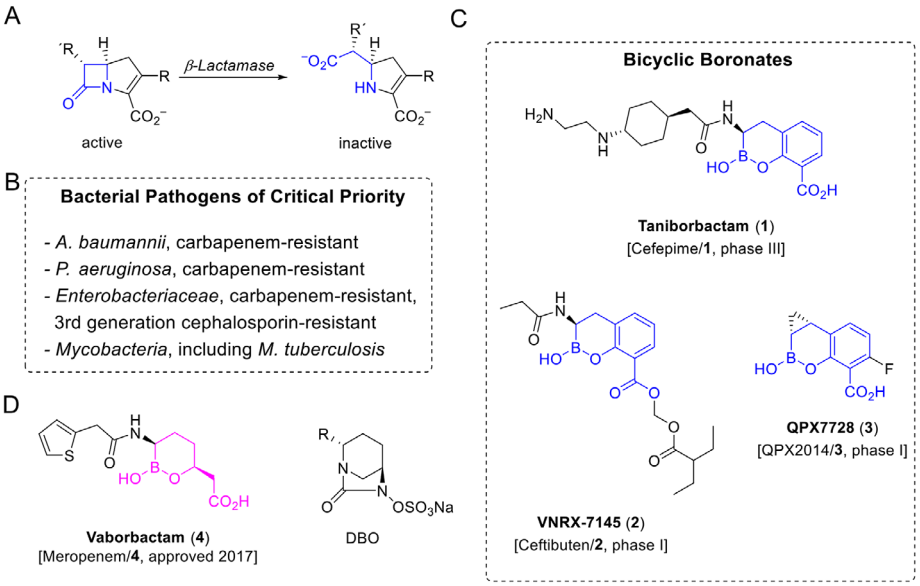

Figure 1. A) Enzymatic inactivation of carbapenems. B) Bacterial pathogens of critical priority according to the WHO. C) Most relevant bicyclic boronate inhibitors under clinical development. D) Chemical structure of vaborbactam that is the first boron-based β-lactamase inhibitor approved by the food and drug administration (FDA) and general structure of 1,6-diazabicyclo[3.2.1]octane (DBO) inhibitors. The combination therapy and the development state are indicated in brackets.

β-lactam antibiotics (penicillins, cephalosporins, monobactams, and carbapenems), which compromise 70% of all antibacterial drugs in clinical use.[21–23] These life-saving drugs are safe, very effective, and well tolerated by most patients, with only few cases of allergic reactions.[24] The mechanism of action involves inhibition of the growth of the bacterial wall, specifically the biosynthesis of the peptidoglycan catalyzed by PBPs (penicillin-binding proteins), which imparts rigidity to this essential structure for bacterial survival.[25] The alteration of the natural balance between the synthesis of peptidoglycan and its hydrolysis, which is catalyzed by murein hydrolases, in the regeneration of the bacterial wall is responsible for the bactericidal effect.

The utility of β-lactam antibiotics is being threatened by the ever-increasing production and dissemination worldwide of β-lactamases.[26,27] These enzymes confer resistance to β-lactam antibiotics through hydrolysis of the β-lactam ring to afford inactive products, thus preventing the inhibition of their therapeutic target, i.e., PBPs (**Figure 1**A). This inactivation process is one of the most relevant resistance mechanisms in Gram-negative bacteria, including the multidrug-resistant pathogens highlighted by the WHO, namely, *Acinetobacter baumannii*, *Pseudomonas aeruginosa*, and *Entereobacteriaceae* (Figure 1B).[28] Among the different types of β-lactamase inhibitors, significant effort is currently being devoted to the development of compounds with an ultrabroad-spectrum activity, i.e., activity against the four types of β-lactamase enzymes, which are characterized as having quite distinct hydrolytic capabilities. This goal has proven to be challenging given the variety of structural topologies of these enzymes and the markedly different mechanisms of action of the serine-based enzymes when compared with the zinc-dependent hydrolases. In particular, the search for efficient inhibitors against the metallo-dependent enzymes, for which effective therapies in clinical practice are currently not available, is one of the field's biggest unmet needs. The search for ultrabroad-spectrum inhibitors that are able to inhibit serine- and metallo-β-lactamase enzymes is an emerging area in antibacterial drug discovery.

The present article is focused on the therapeutic potential of recently developed combination therapies in which the latest bicyclic boronates (monoester form) are used, specifically taniborbactam (formerly VNRX-5133, **1**), the orally bioavailable inhibitor VNRX-7145 (**2**) and QPX7728 (**3**), which are in advanced clinical development (Figure 1C). These resistance breakers are the present hope against β-lactamase-producing carbapenem-resistant superbugs that produce either serine- or/and metallo-β-lactamase enzymes. In order to gain an insight into the scope of the bicyclic boronates currently under clinical study, this article also provides a brief overview of the susceptibility spectrum of the most recent combination therapies approved by the FDA involving other types of β-lactamase inhibitors, such as vaborbactam and 1,6-diazabicyclo[3.2.1]octanes (DBOs) (Figure 1D). Finally, the molecular basis of the ultrabroad-spectrum efficacy of taniborbactam and QPX7728 is also discussed based on the available crystal structures of the enzyme complexes and the Molecular Dynamics (MD) simulation studies discussed here.

2. β-Lactamases: Classes and Mechanisms

The overuse and misuse of β-lactam antibiotics over the last 80 years, together with the intrinsic evolutionary character of bacteria as a response to exposure to hostile environments, has led to the development of a huge number of β-lactamase enzymes. According to the Beta-lactamase database, ≈5000 β-lactamases have been identified to date and these are classified into four groups (A–D) based on their sequence identities.[29–32] These enzymes have quite distinct hydrolytic capabilities and are structurally diverse, with the most frequent classes being A (≈32%) and C (≈30%), followed by D (≈20%), and B (≈14%).[29]

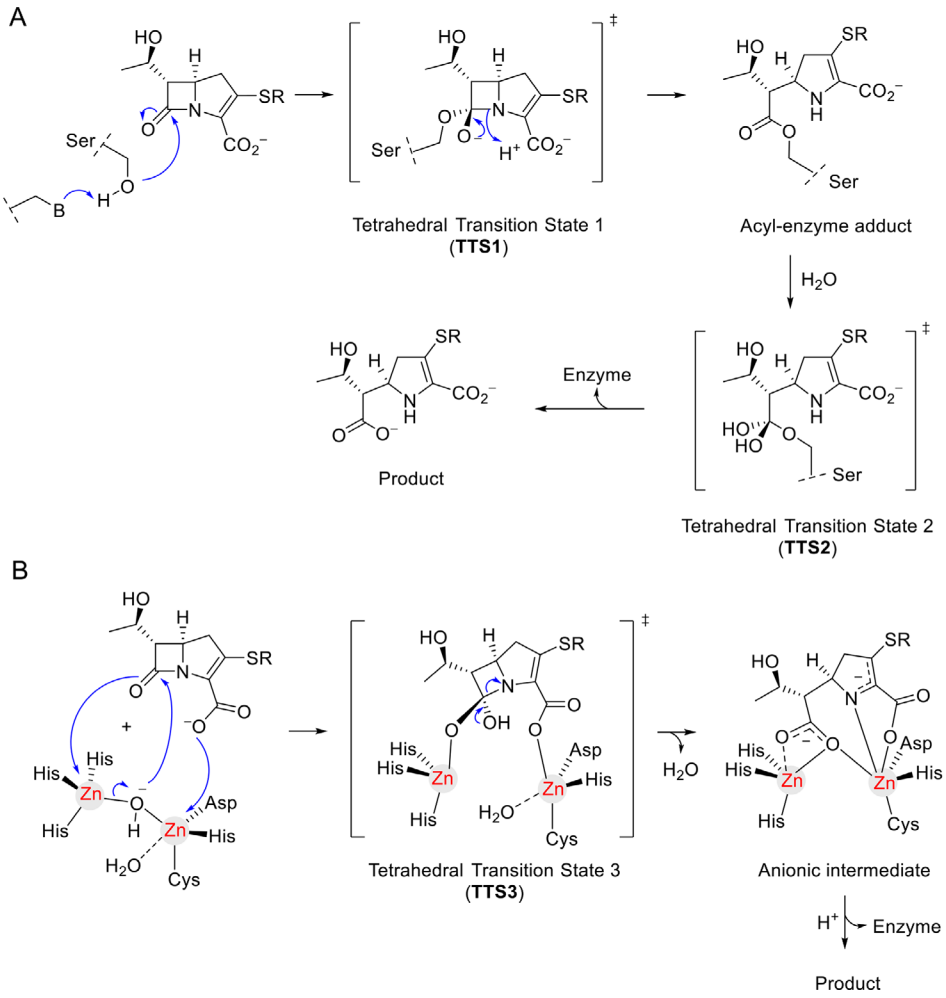

Figure 2. Enzymatic hydrolysis of carbapenems catalyzed by A) serine-β-lactamases and B) metallo-β-lactamases. R = carbapenem side chain.

Classes A, C, and D are serine-β-lactamase enzymes that hydrolyze the β-lactam antibiotic in a covalent-catalyzed process that involves the formation of an acyl-enzyme adduct using a catalytic serine residue, which behaves as the reactive nucleophile, and an active site residue that acts as a general base (lysine, carboxylated lysine or glutamate) (**Figure 2**A).[33,34] The mechanism involves two steps. i) The formation of a tetrahedral transition state 1 TTS1 that will be stabilized by strong hydrogen bonding interactions with the bottom part of the active site (the oxyanion hole). ii) The deacylation process by hydrolysis of the acyl-enzyme adduct through the formation of the tetrahedral transition state 2 TTS2.

Although the mechanism of action of the three types of serine-β-lactamases is globally similar, the structural differences between these species are very relevant and explain their quite distinct hydrolytic capabilities and substrate preferences. Thus, class A enzymes show quite diverse activity since, even though they typically hydrolyze penicillins (in fact they are historically known as penicillinases), some of their variant enzymes have evolved to hydrolyze narrow- and expanded-spectrum cephalosporins (SHV-2, TEM-10, CTX-M, GES-1) and others even hydrolyze carbapenems (KPC, SME, IMI, NMC-A, GES-2).[35,36] Class C enzymes mainly hydrolyze cephalosporins (AmpC, CMY, ACT-1, DHA, FOX). The most relevant examples of this group are the chromosomally encoded AmpC enzymes that inactivate most cephalosporins, including expanded spectrum cephalosporins (ceftazidime, cefotaxime, ceftriazone) and cephamycins (cefoxitin). Although the basal expression of AmpC-type enzymes is usually low, in most clinical isolates high levels can be induced by exposure to β-lactam antibiotics and/or by constitutive expression.[37] The AmpC-type enzymes make the bacterium intrinsically resistant to most cephalosporins. For *P. aeruginosa*, AmpC enzymes are known as PDC (*Pseudomonas*-derived cephalosporinase) and these can be induced in most clinical isolates by β-lactam antibiotics.[38] Class D enzymes (oxacillinases, OXA) hydrolyze penicillins and cloxacillin. However, OXA-type enzymes have also evolved to inactivate narrow-spectrum cephalosporins (OXA-1, OXA-10), expanded-spectrum cephalosporins (OXA-13, OXA-17) or even carbapenems (OXA-23, OXA-24/40, OXA-48), which are known as carbapenem-hydrolyzing class D β-lactamases.[31,39–47]

Unlike serine-β-lactamases (A, C, and D), class B enzymes inactivate β-lactam antibiotics through a completely distinct mechanism that does not involve the formation of ligand-enzyme adducts (Figure 2B). Instead, these enzymes catalyze the hydrolysis of the β-lactam bond using a hydroxide anion as

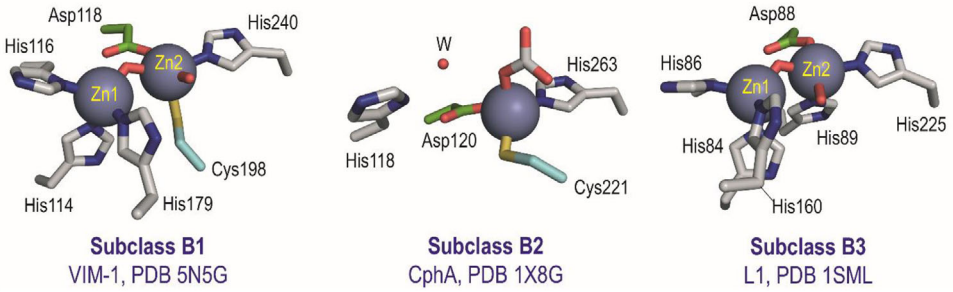

Figure 3. Close view of the active site observed in X-ray crystal structures of β-lactamases of subclasses B1, B2, and B3. Structures of VIM-1 from *P. aeruginosa* (PDB 5N5G), CphA from *Aeromonas hydrophyla* (PDB 1×8G) and L1 *Stenotrophomonas maltophilia* (PDB 1SML) in the wild-type forms are shown. Note how B1 and B3 subclasses are di-zinc-dependent enzymes that have a hydroxide anion bridging the two cationic centers and a common Zn1 site arrangement (His-His-His triad). By contrast, only one catalytic Zn^{2+} ion is involved in the B2 subclass. A carbonate ion coordinated to the metal is observed in PDB 1×8G.

a nucleophile (noncovalent catalysis).[48–56] Class B enzymes are divided into three subclasses (B1, B2, and B3) based on primary amino acid sequence homology, which is relatively low between subclasses (<20%) but significantly higher within a subclass. The B1 and B3 subclasses, which are the most abundant of the three, exhibit a broad-spectrum activity as they can hydrolyze penicillins, cephalosporins, and carbapenems. All B1 and most of B3 enzymes are di-zinc-dependent hydrolases. By contrast, the B2 enzymes are mono-zinc-dependent hydrolases that specifically hydrolyze carbapenems and display poor hydrolytic capacity against penicillins and cephalosporins. For the dinuclear enzymes (B1 and B3 subclasses), the hydroxide anion is bridged by the two Zn^{2+} ions, which are in close proximity to one another (**Figure 3**). One Zn^{2+} ion is coordinated to three histidine residues (Zn1 site, tetrahedral) and the other ion is bound to a water molecule and three residues (for B1 subclass, Asp-Cys-His; and for B3 subclass, Asp-His-His) (Zn2 site, bipyrimidal). It has been proposed that the β-lactam antibiotic hydrolysis process is initiated by coordination of its carboxylate group to the Zn2 site and of its carbonyl group to the Zn1 site. This coordination triggers the nucleophilic attack of the hydroxyl group located between the two ions, thus leading to the tetrahedral transition state 3 TTS3 and the cleavage of the C—N bond (Figure 2B). An anionic intermediate is then generated and subsequently protonated to afford an enzyme/product complex before product release.[57] Based on X-ray crystal structures of NDM-1 in complex with hydrolyzed imipenem and meropenem, as well as NMR monitoring of the reaction process, significant differences in the hydrolysis of carbapenems catalyzed by metallo-β-lactamases were identified compared with penicillins and cephalosporins.[58] The structures of two NDM-1/intermediate complexes (PDBs 5YPK and 5YPI) and the NDM-1/product complex (PDB 5YPL) captured revealed that, in contrast to penicillin and cephalosphorin hydrolysis (PDBs 4EYB and 4EYF),[55] the carbapenem hydrolysis mechanism would involve intermediate complex lacking of a bridging water molecule between the two Zn(II) centers. The final protonation of the hydrolyzed carbapenem intermediate would take place by reaction with a bulky water molecule located in the β-face.

Among the three subclasses, the B1 enzymes are the most abundant and these include the clinically relevant and transferable IMP-, VIM-, and NDM-type enzymes. These hydrolases are the most directly related to β-lactam antibiotic resistance because they are widely found in the deadly pathogens *A. baumannii*, *P. aeruginosa*, and *Enterobacteriaceae*.[59,60] The B2 enzymes are chromosomally encoded and characterized by a bipyramidal coordination of the catalytic Zn^{2+} ion as the Zn2 site arrangement.[48,61] In this case, the nucleophilic hydroxide anion would be generated by deprotonation of the bridging water molecule between the aspartate residue of the zinc coordination sphere and a histidine residue in the vicinity (Asp120 and His118, respectively, in PDB 1×8G, Figure 3).[62] It has been suggested that one of the latter two residues might act as a general base. The B2 subclass enzymes are inhibited when a second Zn^{2+} ion binds to the Zn1 site.[63] CphA and Sfh-I are the most relevant examples of this enzyme subclass.

3. Carbapenemases: The Nightmare of Anti-Infective Therapies Based on β-Lactam Antibiotics

Despite being the least common β-lactamases in deadly pathogens, class B enzymes represent a huge risk to hospitalized patients because i) they can potentially confer extremely broad-spectrum resistance to antibiotics as—with the exception of monobactams—they can hydrolyze virtually all β-lactam antibiotics, and ii) clinically approved inhibitors are not currently available. In addition, the extensive knowledge achieved over the years on the inhibition of serine-β-lactamases, which will be briefly summarized in Section 4, is of little relevance in the search for new inhibitors against these zinc-dependent hydrolases. Thus, there are marked differences between these two types of enzymes, both in the mechanism of action and the structural topology, which hinders the development of effective inhibitors based on previous scaffolds.[60,64–66]

Nowadays, there is a great deal of concern about the impact of the infections caused by carbapenem-resistant *A. baumannii*, *P. aeruginosa*, and *Enterobacteriaceae* that are frequently found in hospitalized patients fitted with invasive devices or exposed to extended antibiotic regimens.[67–70] Of particular concern is the global incidence of class A carbapenemases, such as KPC, SME, IMI, NMC-A, and GES-2, carbapenem-hydrolyzing class D β-lactamases, such as OXA-23, OXA-24/40, and OXA-48,

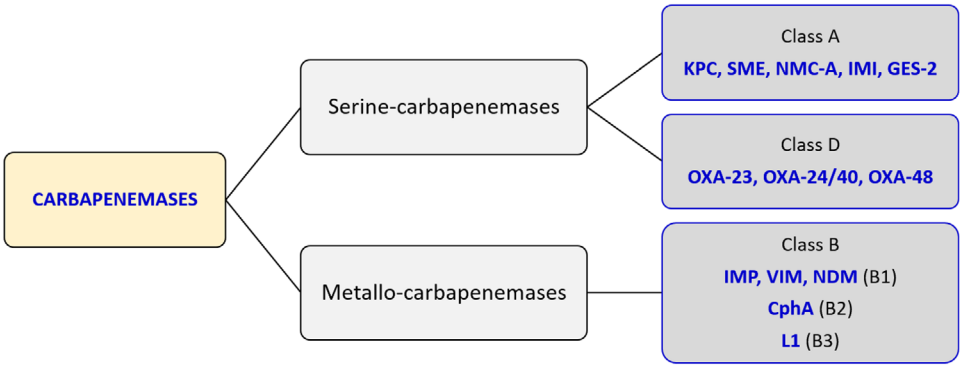

Figure 4. Most relevant carbapenemases widely found in multidrug-resistant pathogens *A. baumannii*, *P. aeruginosa*, and *Enterobacteriaceae*.

as well as metallo-β-lactamases such as IMP, VIM, and NDM (**Figure 4**). The ever-increasing appearance and dissemination in clinical settings of these types of strains, which are mostly encoded by plasmids, is worrisome since it significantly narrows the therapeutic options and, in some cases, solutions are not available. This issue is further exacerbated by the existence and spread of bacterial strains that coproduce serine- and metallo-carbapenemases. Thus, i) class B enzymes hydrolyze approved serine-β-lactamase inhibitors such as avibactam, and efficient inhibitors against them are not clinically available,[71] and ii) numerous examples of clinical isolates of *Klebsiella pneumoniae* strains that coexpress NDM-1 and OXA-type enzymes have already been found worldwide (India, Nepal, Italy, Korea, United Arab Emirates, Switzerland).[72–79] It is therefore not surprising that the development of carbapenemase inhibitors with an ultrabroad-spectrum activity, i.e., effective against both metallo- and serine-β-lactamases, has become a flourishing research area in drug discovery in recent years.

4. Overview and Spectrum Susceptibility of Non-Boron-Based β-Lactamase Inhibitors

The most relevant β-lactamase inhibitors, either in clinical use or at different stages of development, are summarized in **Figure 5**. Clavulanic acid (**4**) and the penicillin-based sulfones sulbactam (**5**) and tazobactam (**6**), which were the first to be introduced in clinic in combination with various penicillins (amoxicillin, ampicillin, piperacillin, ticarcillin) as well as more recently with fourth and fifth generation cephalosporins (cefepime, ceftolozane) are only effective against bacterial strains that harbor extended-spectrum-β-lactamases (ESBLs, class A).[80,81] None of these combinations, including the recently developed enmetazobactam (**7**, formerly AAI101)/cefepime,[82] are useful against strains that produce the most relevant serine- and metallo-carbapenemases or against class C cephalosporinases (Figure 4).

A huge breakthrough in β-lactamase inhibition was the development of 1,6-diazabicyclo[3.2.1]octanes (DBOs) that was triggered by the identification of its parent inhibitor, avibactam (**8**), which was approved in 2014 by the FDA in combination with ceftazidime.[83–85] Avibactam efficiently restores the bactericidal activity of ceftazidime against infections caused by bacterial strains producing class A carbapenemases (KPC-type), class C cephalosporinases (AmpC-type), as well as some class D enzymes (OXA-48) (**Table 1**). Unfortunately, the combination avibactam/ceftazidime is ineffective against relevant strains harboring carbapenem-hydrolyzing class D β-lactamases, such as OXA-23 and OXA-24/40, which are widely found in *P. aeruginosa* and *A. baumannii*, as well as Enterobacteriaceae-producing metallo-carbapenemases, such as NDM-1, IMP-1 and VIM-1/VIM-2. Recently, avibactam in combination with aztreonam and metronidazol has opened new therapeutic opportunities for the treatment of infections caused by Gram-negative bacteria producing metallo-β-lactamases, in particular, intra-abdominal infections and nosocomial pneumonia.[86–87] This therapy, which exploits the stability of aztreonam against class B enzymes and is currently under phase III of clinical development, is efficient against the vast majority of Enterobacteriaceae and particularly attractive for patients with a history of allergy to other β-lactam antibiotics. However, this treatment is not suitable for infections caused by Gram-positive or anaerobic bacteria, since aztreonam is inefficient against them.[88]

The discovery of avibactam (**9**) triggered a frantic race to expand its spectrum of activity by modification of its DBO scaffold. In particular, significant attention has been devoted to expand avibactam's activity against bacterial strains that express class D carbapenemase OXA-23 and OXA-24/40 enzymes. Efforts were initially focused on modifications of the side chain (primary amide group), either directed to introduce into the scaffold extra binding interactions with the active site and/or to improve their pharmacological properties. This research led to the discovery of relebactam (**10**), which was approved in 2019 by the FDA in combination with imipenem and cilastatin,[89,90] followed by zidebactam (**11**, formerly WCK 5222)[91–93] and nacubactam (**12**, formerly RG6080, OP0595),[94–96] which are both under phase I clinical studies in combination with cefepime and meropenem, respectively. Unlike the other DBO inhibitors, nacubactam has a dual mode of action because, in addition to being a serine-β-lactamase inhibitor, it also has bactericidal activity by targeting PBP2 in *Enterobacteriaceae*.[96–98]

The most meaningful progress in the development of DBO inhibitors occurred with the rigidification and functionalization of the six-membered ring. This type of modification provided a solution to one of the field's long-pursued unmet needs, namely to expand the inhibitory range of these compounds to include class D β-lactamases, such as OXA-23 and OXA-24/40, in the list of serine β-lactamases that can be blocked (Table 1). Unlike

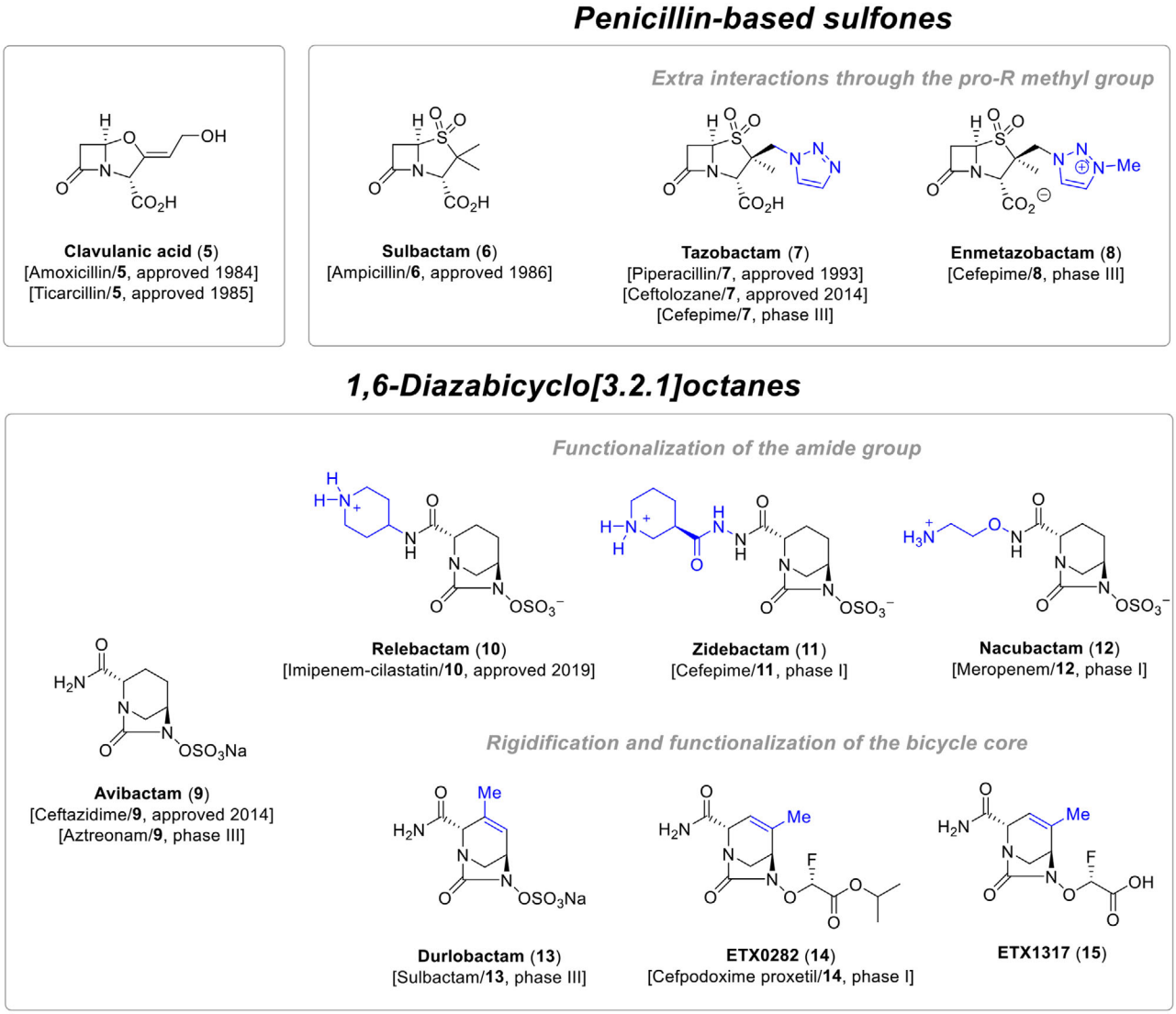

Figure 5. Clavulanic acid (**5**), most relevant examples of penicillin-based sulfones and 1,6-diazabicyclo[3.2.1]octanes. The combination therapy and the development state are indicated in brackets. The chemical modifications in the parent inhibitors, sulbactam and avibactam, that have resulted in subsequent analogs are highlighted in blue.

other β-lactamases, the latter class D carbapenemases have a rigid and apolar tunnel-like entrance, which is composed of a methionine and a tyrosine or phenylalanine residue, that facilitates exquisite control of the substrate conformation for the serine-catalyzed hydrolysis, thus enhancing the carbapenemase activity.[99] The most prominent inhibitor, which was developed by Entasis Therapeutics, is durlobactam (**13**, formerly ETX2514) and together with sulbactam (**5**) this proved to be an excellent therapeutic candidate for the treatment of infections caused by multidrug-resistant Acinetobacter spp.[100–102] The combination durlobactam/sulbactam is currently under phase III clinical studies. The same company also developed ETX0282 (**14**), an oral prodrug of another relevant DBO analog ETX1317 (**15**), which is a regioisomer of durlobactam (**13**) in which the sulfate moiety has been replaced by an (*R*)-2-fluoroacetate group. ETX0282 (**14**) in combination with cefpodoxime proxetil, which is a prodrug of cefpodoxime approved for the treatment of antibiotic-resistant Enterobacteriaceae urinary tract infection, is a promising oral therapy for infections caused by ESBL-producing and carbapenem-resistant *Enterobacteriaceae*.[103–106] Undoubtedly, the broad-spectrum of activity of durlobactam (**13**) and ETX0282 (**14**)—or its active form ETX1317 (**15**)—represents a huge advance in restoring the efficacy of carbapenems in infections caused by the WHO priority pathogens. However, like avibactam these compounds are also inefficient against metallo-β-lactamases (Table 1).

5. Bicyclic Boronates: The Present Hope Toward "Pan-β-Lactamase Inhibitors"

In general, the ability of boronic acids to change their hybridization state between sp2 (trigonal) and sp3 (tetrahedral) forms

Table 1. Spectrum of activity of DBO inhibitors among the fourth classes of β-lactamase enzymes.

Inhibitor	Class A	Class C	Class B	Class D
Avibactam (**9**)	Yes	Yes	No	Some
	ESBL, KPC	AmpC-type	–	OXA-10, OXA-48
Relebactam (**10**)	Yes	Yes	No	No
	ESBL, KPC	AmpC-type	–	–
Zidebactam (**11**)	Yes	Yes	No	No
	ESBL, KPC	AmpC-type	–	–
Nacubactam (**12**)	Yes	Yes	No	No
	ESBL, KPC	AmpC-type	–	–
Durlobactam (**13**)	Yes	Yes	No	Yes
	ESBL, KPC	AmpC-type	–	OXA-1, OXA-10, OXA-23, OXA-24/40, OXA-48
ETX0282 (**14**)	Yes	Yes	No	Yes
	ESBL, KPC	AmpC-type	–	OXA-1, OXA-10, OXA-23, OXA-24/40, OXA-48

in aqueous environments makes them good mimetics of the transition state for enzymes using amides, esters or lactams as substrates.[107] This feature and the improved pharmacokinetics profile of the corresponding derivatives are attractive properties that have been exploited in drug development and resulted in several approved drugs. Good examples are bortezomid (Velcade, FDA approved in 2005)[108] and ixazomid (Ninlaro, FDA approved in 2015),[109] which are proteasome inhibitors used for the treatment of myeloma, and tavaborole (Kerydin, FDA approved in 2014),[110] which is a Leucyl-tRNA synthetase inhibitor employed for the treatment of onychomycosis (a fungal infection).

The investigations into the potential of boronic acids in the β-lactamase inhibition field emerged after it was demonstrated that boric acid and subsequent diverse phenylboronic acids inhibit serine-β-lactamase enzymes.[33,111–113] These compounds are considered good transition state analogs of TTS1 and TTS2, for which their capacity to be in equilibrium between their sp2/sp3 forms is also crucial to maximize their affinity during both the binding and inhibition processes (Figure 2). Thus, in the Michaelis complex formation step the sp2 form, which usually predominates at neutral pH,[112] can mimic the carbonyl group of β-lactam antibiotics as they also have an sp2 geometry.[33] Once this complex is established, the ability of the boronic acid to tune to the sp3 form provides a good mimetic of the high-energy tetrahedral transition states TTS1 and TTS2 in the serine-β-lactamase mechanism, as well as TTS3 in the conversion catalyzed by the metallo-β-lactamase enzymes (Figure 2). This effective "sp2/sp3 equilibrium process" is consistent with the high k_{on} and low k_{off} values experimentally observed in compounds of these types.[114,115]

Initially, the main bottleneck for the use of boronic acids in this field was their potential side effects due to the additional inhibition of mammalian serine proteases.[116] However, the introduction of cyclic boronates (1,2-oxaborinan-2-ol and 3,4-dihydro-2*H*-benzo[*e*][1,2]oxaborinin-2-ol) was a turning point in the field due to their greater selectivity against β-lactamase enzymes (**Figure 6**). The latter characteristic is mainly caused by the restricted conformation of this chemical scaffold, which would not fit in the smaller active sites of the serine proteases as they have been exquisitely designed for transforming more flexible substrates. As for the penicillin-based sulfone inhibitors [sulbactam (**6**), tazobactam (**7**), enmetazobactam (**8**)], the presence in the scaffold of a carboxylate group in the α-position to the cyclic oxygen atom proved to be pivotal for anchoring to the active site of the serine-β-lactamase enzymes, either through electrostatic and/or hydrogen bonding interactions with key polar residues, as well as for coordination to the Zn^{2+} ion of the metallo-β-lactamases.

5.1. Taniborbactam (VNRX-5133)

The inspiration for the design of inhibitors based on cyclic boronates arose from the X-ray structure of TEM-1 β-lactamase from *Escherichia coli* covalently modified by (1*R*)-1-acetamido-2-(3-carboxy-2-hydroxyphenyl)ethylboronic acid (PDB 1ERQ, 1.9 Å) reported by Ness et al. (Figure 6A).[117] In the structure, the strong hydrogen bonding interaction observed between the phenol group in the modified ligand and the oxygen atom of the catalytic serine seems to induce a suitable arrangement of the ligand for coordination to the catalytic Zn^{2+} ion through its phenol and carboxylate moieties. This hypothesis led Burns et al.[118] in 2010 at Protez pharmaceuticals, a subsidiary of Novartis, to develop the first boron-based compounds, specifically the bicyclic boronates, that were able to inhibit both serine- and metallo-β-lactamase enzyme. Further development at Venatorx Pharmaceuticals, with particular attention paid to the optimization of the flexible side chain of the ligand, led to the discovery of taniborbactam (**1**, formerly VNRX-5133), an injectable pan-β-lactamase inhibitor (Figure 1C).[119–122] In parallel, Rempex Pharmaceuticals developed diverse monocyclic boronates that allowed the identification of vaborbactam (**4**, formerly RPX7009), which is the first boron-based β-lactamase inhibitor approved by the FDA in combination with meropenem (2017, vabomere) for the treatment of complicated urinary tract infections (Figure 1D).[123,124] The European Medicines Agency also approved the vaborbactam/meropenem combination for the treatment of intra-abdominal infections and hospital-acquired pneumonia.[125]

The most remarkable feature of varborbactam is its strong capacity in restoring the activity of carbapenems against strains that produce ESBLs, especially KPC-producing *Enterobacteriaceae,* with K_i values in the nanomolar range (**Table 2**).[123] This compound provides highly stable adducts, the tridimensional structure of which was solved by X-ray crystallography (PDB 6TD0,[126] 0.99 Å). Vaborbactam is a reversible inhibitor with a remarkable very slow off-rate constant (≈40 μs^{-1}) and a corresponding residence time of ≈7 h against KPC-enzymes.[127] A substantially faster release of the vaborbactam bound form occurs against other serine-β-lactamases. In vitro studies with KPC-producing strains showed that vaborbactam reduces the minimum inhibitory concentration (MIC) values of meropenem by ≥64-fold. This compound also efficiently inhibits other β-lactamases of classes A (CTX-M, SHV, TEM-10) and C (*Enterobacter cloacae* cephalosporinase P99, *K. pneumoniae* CMY-2) in the 10×10^{-9}–100×10^{-9} M range but it does not have bactericidal activity (Table 2).[128] Unfortunately, vaborbactam lacks

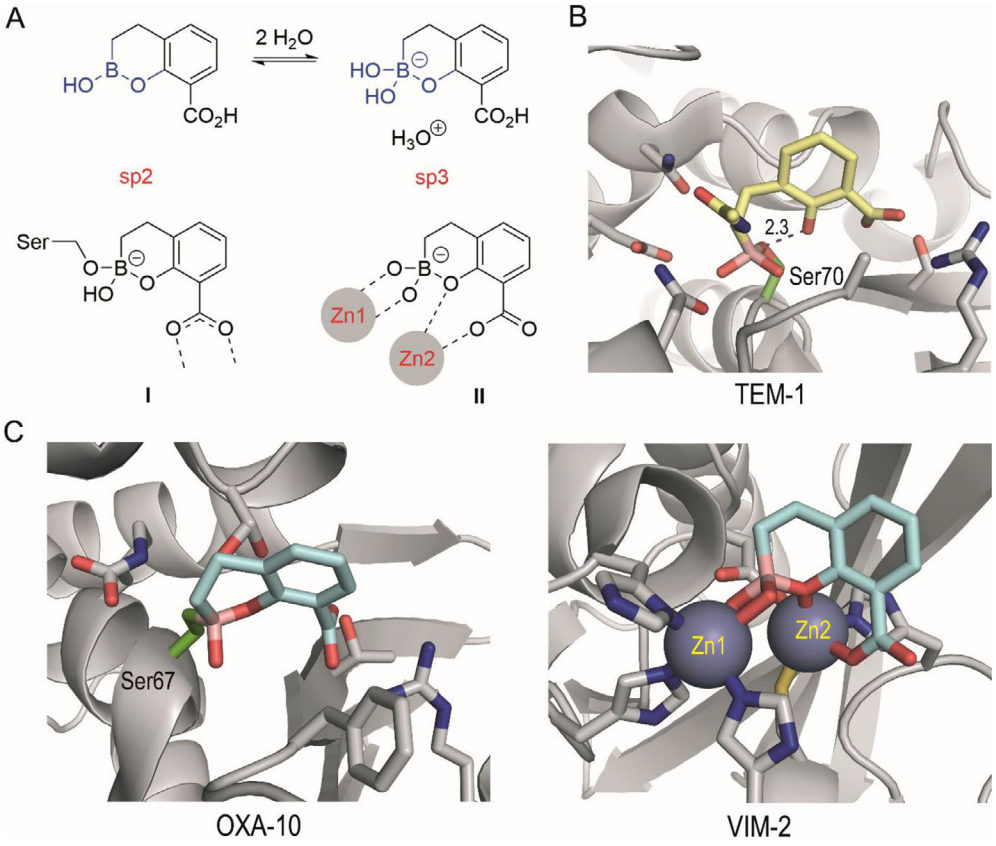

Figure 6. The sp3 form of cyclic boronates is key for the inhibition of both serine and metallo-β-lactamases. A) sp2/sp3 equilibrium forms of 3,4-dihydro-2*H*-benzo[*e*][1,2]oxaborinin-2-ol derivatives and schematic representation of the resulting serine adduct I and di-zinc-complex II. B) Detailed view of the active site of β-lactamase TEM-1 from *E. coli* covalently modified by (1*R*)-1-acetamido-2-(3-carboxy-2-hydroxyphenyl)ethylboronic acid (PDB 1ERQ,[117] 1.9 Å). Note how the phenol group is in close contact with the catalytic Ser70 (2.3 Å). C) Tridimensional structure of I and II observed in PDB 6RTN[130] (OXA-10 from *P. aeruginosa*) and 6SP7[131] (VIM-2 from *P. aeruginosa*). Only the bicyclic boronate core of the ligand (cyan) is shown.

clinical utility for the treatment of infections caused by bacterial pathogens that produce carbapenemases of classes B and D, as it proved to be a weak inhibitor of these enzymes (µM range). Among the B1 subclass, its inhibitory activity against the IMP-1 enzyme stands out when compared to VIM-1/VIM-2 and NMD-1, which are lower by a factor of around 5.

The bicyclic architecture of taniborbactam (**1**) has proven to be key in achieving nanomolar activity against class B enzymes because of the conformational restraints induced by the fused aromatic ring that preorganizes the ligand for binding. This bicyclic boronate efficiently inhibits the B1 subclass enzymes VIM and NDM, with IC_{50} values in the nanomolar range, as well as serine-β-lactamases of ESBLs, OXA-type, and KPC-type (Table 2).[129–131] This outstanding ultrabroad-spectrum activity makes taniborbactam (**1**) an excellent antibiotic partner for the treatment of infections due to carbapenem-resistant pathogens with distinct mechanisms of action, including carbapenem-resistant *Enterobacterales* and carbapenem-resistant *P. aeruginosa*.[132] Taniborbactam (**1**) is the first pan-β-lactamase inhibitor to enter clinical trials that is able to inhibit both metallo- and serine-β-lactamases. Specifically, in combination with cefepime, a fourth-generation cephalosporin, it is currently in phase III studies.

Venatorx Pharmaceuticals Inc. developed an orally bioavailable boron-based β-lactamase inhibitor, VNRX-7145 (**2**), which is a proform of VNRX-5236, a bicyclic boronate derivative structurally related to taniborbactam but with a short side chain (propionamido).[133,134] In combination with ceftibuten, a third generation cephalosporine, VNRX-5236 restores the antibiotic efficacy against ESBLs and carbapenem-resistant *Enterobacterales*, including strains that harbor KPC-type and OXA-type carbapenemases. The combination ceftibuten/VNRX-7145 is currently in phase I clinical development.

Taniborbactam (**1**) is synthesized in six steps from commercially available boronic acid **16** as shown in **Scheme 1**.[118–120] As for the synthesis of other inhibitors based on cyclic boronates such as vaniborbactam (**4**), Matteson's reaction is employed for the double homologation of the boronic acid pinanediol ester intermediate **17**, which is readily prepared in two steps by double esterification of **16** to give chloride **19**. SN2 reaction of chloride **19** with lithium bis(trimethylsilyl)amide and subsequent coupling with carboxylic acid **23** using HATU and NMO provide amide **20**. The required acid **23** is prepared in five steps from commercially available carboxylic acid **21**. Finally, treatment of **20** with BCl_3 leads to the deprotection of all functional groups and the formation of the bicyclic core in taniborbactam (**1**).

Table 2. Inhibitory activity [IC_{50} (μM)] of taniborbactam (**1**), vaborbactam (**4**), avibactam (**9**), clavulanic acid (**5**), and tazobactam (**7**) against relevant serine- and metallo-β-lactamase enzymes.

Class	Enzyme	Taniborbactam (**1**)	Vaborbactam (**4**)	Avibactam (**9**)	Clavulanic acid (**5**)	Tazobactam (**7**)
A	TEM-116	0.12[128]	6[128]	NA[a)]	NA	NA
	KPC-2	0.03[131]	0.09[128]	0.06[131]	1.8[131]	1.7[131]
	SHV-5	0.0004[131]	0.44[131]	0.013[131]	0.012[131]	0.015[131]
	CTX-M-15	0.01[131]	0.42[131]	0.003[131]	0.04[131]	0.001[131]
B1	IMP-1	39.8[131]	126[128]	>100[131]	>100[131]	>100[131]
		2.51[130]				
	NDM-1	0.19[131]	631[128]	>100[131]	>100[131]	>100[131]
		0.01[130]				
	VIM-1	0.0079[130]	398[128]	NA	NA	NA
	VIM-2	0.026[131]	316[128]	>100[131]	>100[131]	>100[131]
		0.0005[130]				
B2	CphA	2.51[130]	631[128]	NA	NA	NA
B3	L1	>10[130]	336[128]	NA	NA	NA
C	AmpC	0.301[130]	5[128]	NA	NA	NA
	P99	0.03[131]	0.09[131]	0.016[131]	>100[131]	0.73[131]
	CMY-2	0.007[131]	0.22[131]	0.007[131]	>100[131]	0.41[131]
D	OXA-1	0.16[131]	7.9[131]	0.04[131]	0.12[131]	0.43[131]
	OXA-48	0.42[131]	25[128]	0.55[131]	30[131]	0.55[131]
		0.54[130]	38.8[131]	0.55[131]	30[131]	0.55[131]

[a)] NA = Not available.

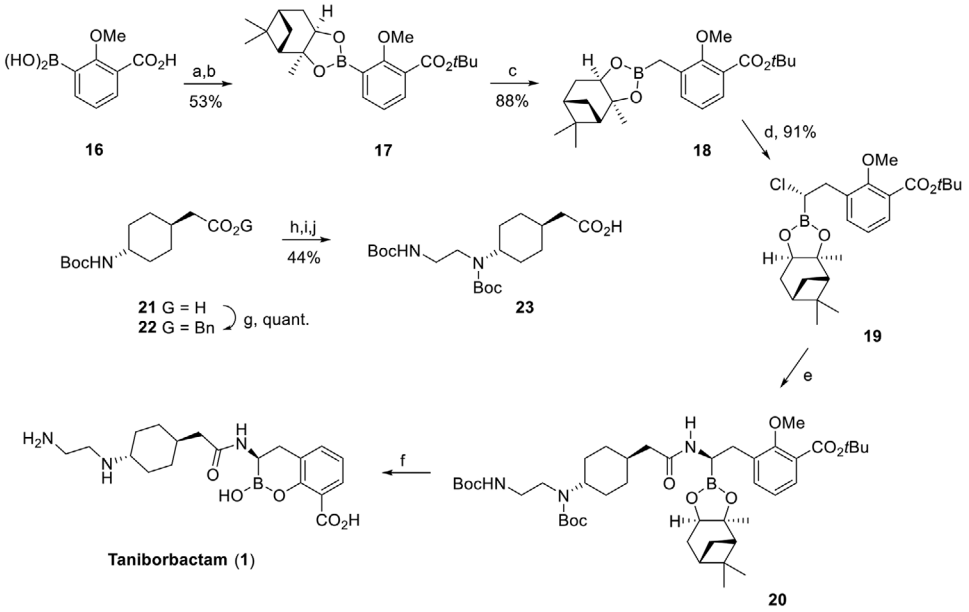

Scheme 1. Synthesis of taniborbactam (**1**). Reagents, and conditions: (a) Isobutene, H_2SO_4 (c), dioxane, RT. (b) (+)-pinanediol, THF, RT. (c) CH_2ClI, *n*BuLi, THF, −100 °C to RT., CH_2Cl_2, −78 °C. (d) 1. CH_2Cl_2, *n*BuLi, THF, −100 °C. 2. $ZnCl_2$, −100 °C to −10 °C. (e) 1. LHMDS, THF, −20 °C to RT. 2. **23**, HATU, NMO, *N*,*N*-dimethylacetamide, RT. (f) BCl_3, CH_2Cl_2, −78 °C. (g) BnBr, K_2CO_3, DMF, RT. (h) CH_2Cl_2, HCl (4 M in dioxane), RT. (i) 1. Et_3N, $(CH_2Cl)_2$, RT. 2. HOAc, *N*-Boc-aminoacetaldehyde, $NaBH(OAc)_3$, RT. (j) 1. Boc_2O, Et_3N, CH_2Cl_2, RT. 2. H_2 (g), Pd/C (10%), EtOAc, RT.

5.1.1. Molecular Basis of Taniborbactam's Efficacy against Class B1 Metallo-β-Lactamases

A differentiating feature between taniborbactam (**1**) and vaborbactam (**4**), beyond the markedly superior inhibitory capacity of the former against class B enzymes (nanomolar vs micromolar, respectively), is their distinct selectivity between B1 enzymes (Table 2). Thus, while vaborbactam has a modest and similar inhibition of the main B1 enzymes (VIM-1/2, NDM-1, IMP-1), taniborbactam is notably more effective against VIM-1/2 and NDM-1

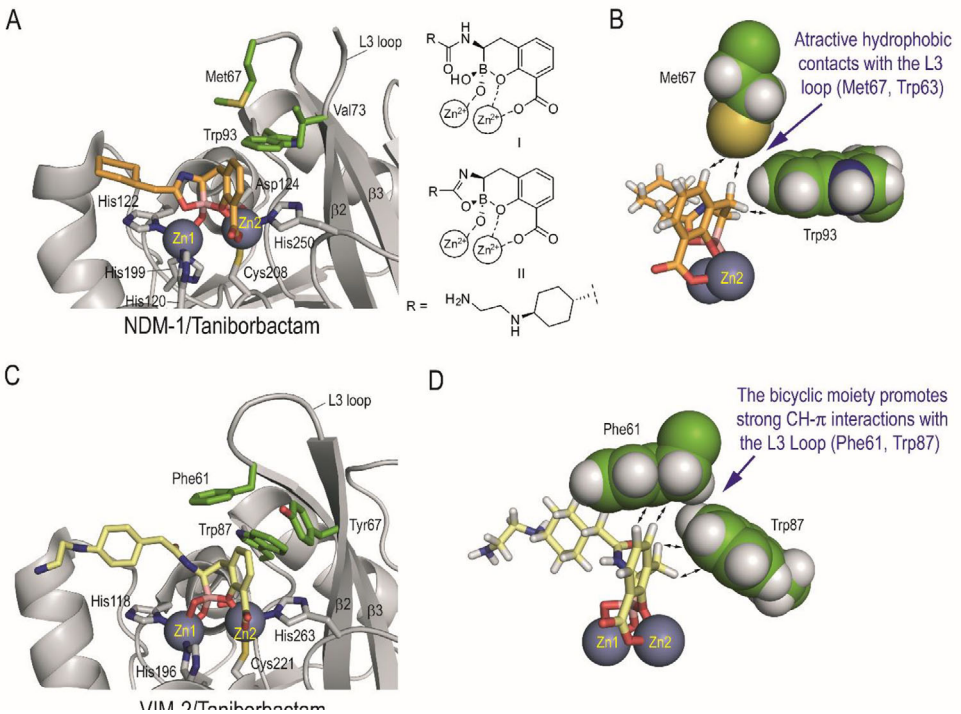

Figure 7. Analysis of the available crystal structures of the B1 enzymes in complex with taniborbactam. A) Crystal structure of NDM-1 from *K. pneumoniae* in complex with taniborbactam (PDB 6RMF,[130] 1.51 Å, chain A). Part of the ligand side chain is not shown since it has not been solved. Two types of enzyme complexes are observed, specifically the bicyclic (I) and the tricyclic (II) boronate complexes. Form I is shown. B,D) Close view of the main hydrophobic contacts between the bicyclic moiety in taniborbactam and the neighboring L3 loop residues (shown as spheres) of NDM-1 (B, Met67 and Trp93) and VIM-2 (D, Phe61 and Trp87). C) Crystal structure of the VIM-2 from *P. aeruginosa* in complex with taniborbactam (PDB 6SP7,[131] 1.80 Å). Relevant side chain residues are shown and labeled. Zn^{2+} ions are shown as spheres.

enzymes. Taniborbactam is around 7- and 1500-fold more potent against VIM-1/2 than NMD-1 and IMP-1, respectively. By contrast, the activity of vaborbactam against the IMP-1 enzyme is about 2.5- and 5-fold higher than for VIM-1/2 and NDM-1 enzymes, respectively.

Analysis of the available crystal structures of the B1 enzymes in complex with taniborbactam reveals important structural differences between them, specifically concerning the hydrophobic pocket that surrounds the bicyclic moiety of the ligand—a difference that might explain these findings (**Figure 7**). The crystal structures of the NDM-1 and VIM-2 enzymes in complex with taniborbactam [PDB 6RMF[130] (1.51 Å) and 6SP7[131] (1.80 Å), respectively] show that the ligand is anchored to the catalytic center through coordination to: i) the Zn1 site via the boronate moiety; and ii) the Zn2 site via the carboxylate group (Figures 7A,C). In both structures the endocyclic oxygen atom in the ligand also interacts with the Zn2 site. For the NDM-1/taniborbactam complex two types of complexes are observed, namely, the bicyclic complex I and the tricyclic complex II (Figure 7A). The latter complex would result from the intramolecular nucleophilic addition of the OH group of the boronate monoester form to the amide group of the side chain. In both complexes the bicyclic ring of taniborbactam is located on the apolar pocket involving the L3 loop and one of the faces of the β2 and β3 sheets. The structural differences in this hydrophobic pocket, as well as the dissimilar arrangement of the L3 loop between the three enzymes, seem to be mainly responsible for the distinct inhibitory potency observed. Thus, for the VIM-2/taniborbactam complex, the bicyclic moiety is deeply surrounded by residues Phe61 and Trp87 to establish strong CH–π interactions with them (Figure 7D). However, for the NDM-1/taniborbactam complex, the position equivalent to Phe61 is occupied by Met67 (Figure 7B). Although the interactions between aromatic rings and the sulfur atoms of the methionine residues are relevant and are commonly found in numerous crystal structures, the bicyclic moiety is less efficiently beset by the enzyme, which might account for its lower affinity against the NDM-1 enzyme.[135–137]

Moreover, the comparison of the crystal structures of IMP-1 from *S. marcescens* (PDB 5EV6, 1.98 Å, wild-type form),[138] NDM-1 from *K. pneumoniae* (PDB 4EYL, 1.90 Å),[55] and the VIM-2/taniborbactam complex reveals that the IMP-1 active site is highly shielded by its L3 loop (**Figure 8**). This tunnel-like architecture of the IMP-1 active site, which is similar to the carbapenemases of class D OXA-23 and OXA-24/40, would make it difficult to achieve binding of rigid systems such as taniborbactam. By contrast, the arrangement of the L3 loop as an active site lid, which is observed in the VIM-2 enzyme, would facilitate the entrance of conformationally constrained ligands, and also promote favorable contacts with them.

In order to gain further insights into these relevant structural differences, the binding modes of vaborbactam and taniborbactam in the active site of VIM-2 were modeled using the Gaussian 09W[140] program package at density functional theory (DFT) level by means of the B3LYP functional, and the enzyme

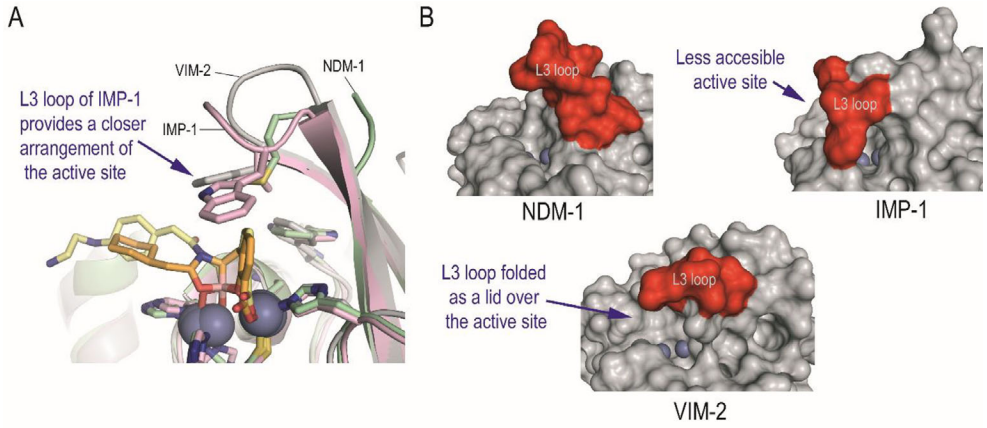

Figure 8. Comparison of the L3 loop arrangement in diverse crystal structures of the B1 enzymes. A) Superposition of the crystal structures of NDM-1/taniborbactam (green, PDB 6RMF[130]), VIM-2/taniborbactam (gray, PDB 6SP7[131]), and IMP-1 from *S. marcescens* (pink, PDB 5EV6[138]). B) Overall view of the crystal structures of NDM-1 (PDB 4EYL[55]), IMP-1 (PDB 5EV6), and VIM-2 (PDB 4NQ2[139]). The L3 loop in all enzymes is highlighted in red. Relevant side chain residues are shown. Zn^{2+} ions are shown as spheres.

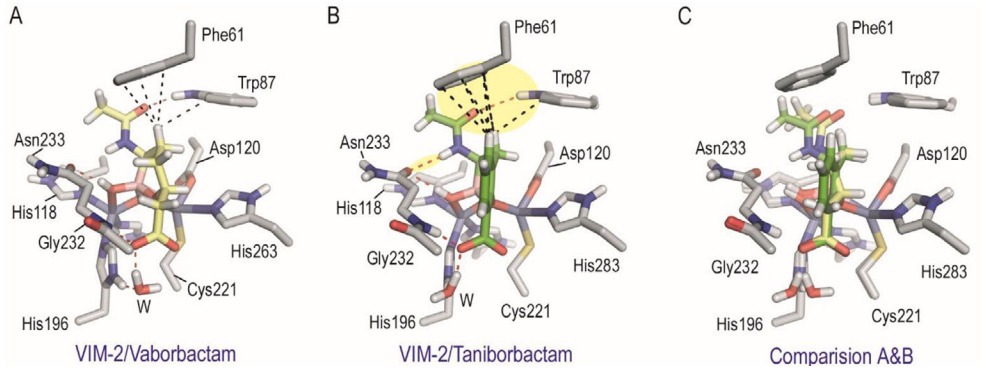

Figure 9. Comparison of vaborbactam and taniborbactam binding mode to VIM-2. Proposed binding mode of A) vaborbactam and B) taniborbactam in the active site of VIM-2 from *P. aeruginosa* obtained by molecular modeling. C) Comparison of (A) and (B). Relevant side chain residues are shown and labeled. Relevant hydrogen bonding and hydrophobic interactions are shown as dashed lines (red and black, respectively). Note how taniborbactam interacts by a strong hydrogen bonding interaction with the Asn233 side chain, which is located in the L10 loop, and also establishes more hydrophobic contacts with Phe61, which is located in the L3 loop.

coordinates determined in PDB 6SP7.[141,142] The standard 6–31G+(d,p)[143,144] basis set was used for C, H, O, S, B, and N, and the LANL2DZ relativistic pseudopotential was used for Zn.[145] The binding mode of taniborbactam with VIM-2 was also modeled as a control to validate the methodology employed. The results with the VIM-2 enzyme showed that the introduction of a fused aromatic ring in the cyclic boronate scaffold facilitated the approach of the amide side chain to the L10 loop (**Figure 9**). As a consequence, a strong hydrogen bonding interaction with the Asn233 side chain was established, which was not observed in the VIM-2/vaborbactam enzyme complex (Figure 9A vs B). In addition, the aromatic ring in taniborbactam also enhanced the CH–π interactions with the residue Phe61 located on the L3 loop. For the vaborbactam/VIM-2 complex, the latter contacts mainly involve the methylene group of the six-membered ring. These two extra interactions might be responsible for the markedly higher affinity of taniborbactam against the VIM-2 enzyme.

Comparison of the available crystal structures of IMP-1, VIM-1/2, and NDM-1 in the unbound form and in complex with inhibitors, shows that the binding of the ligand causes: i) the distancing of both metal centers; and ii) that the latter effect is more pronounced as there are several atoms of the ligand involved in the coordination. Thus, for the unbound forms, the observed range of distances between both Zn^{2+} ions are 3.3–3.6 Å for IMP-1, 3.4–3.8 Å for VIM-1/2, and 3.4–3.8 Å for NDM-1 (Figure S1, Supporting Information). In the latter case, only in few examples distances of up to 4.2 Å are observed, which might be crystallographic artifacts. As expected, similar values are observed for those binary enzyme/ligand complexes where the hydroxyl group bridging both ions is replaced by one atom of the ligand (thiolate). However, for those enzyme/ligand complexes containing phosphates or cyclic boronates coordinated to the two Zn^{2+} ions, the distance observed is significantly greater to accommodate more atoms between them. Thus, for these cases, the common distance range between Zn^{2+} ions is 4.2–4.4 Å for VIM-1/2 and NDM-1 complexes. As a result of the distancing of both metal centers, the loop that surrounds both ions (bottom part of the active site), namely L10, display distinct arrangements to maximize the

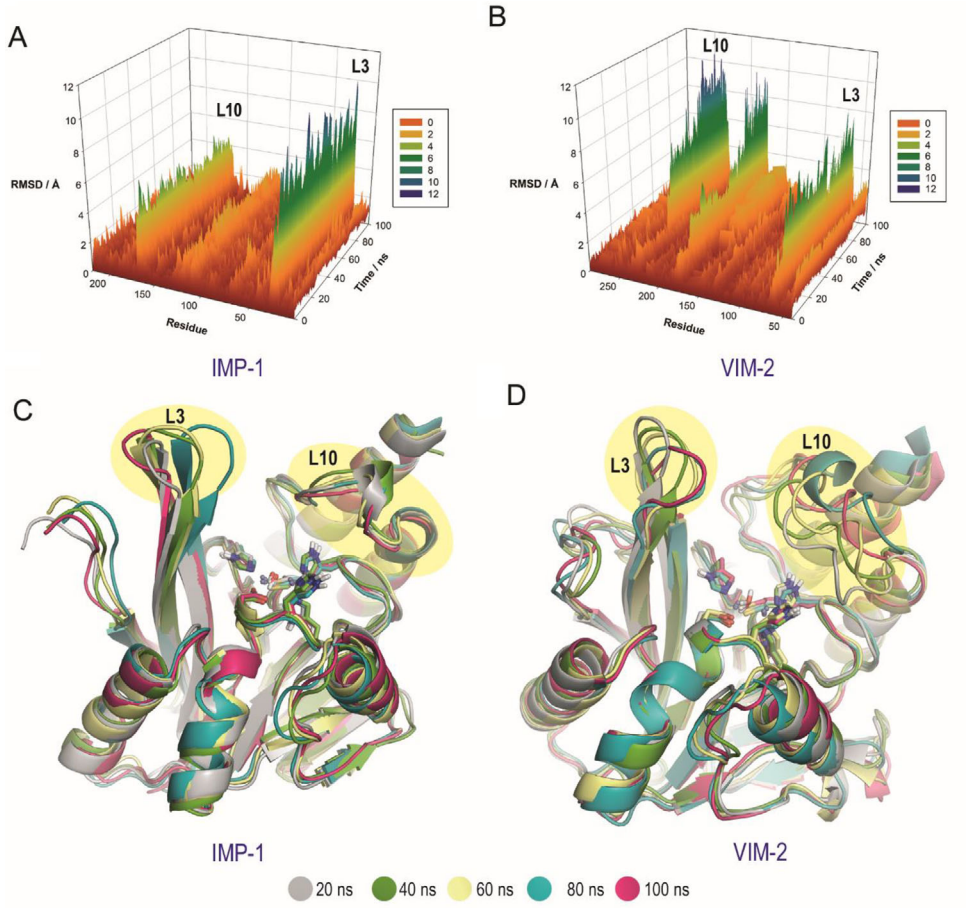

Figure 10. Analysis of the intrinsic shape-changing motions of IMP-1 and VIM-2 enzymes. A,B) RMSD plots for the protein backbone (Cα, C, N, and O atoms) calculated per residue in the wild-type form of IMP-1 from *Serratia marcescens* (A, PDB 5EV6) and VIM-2 from *P. aeruginosa* (B, PDB 5ACU) obtained from MD simulations studies. C,D) Superposition of several snapshots of the IMP-1 (C) and VIM-2 (D) enzymes during 100 ns of simulation. The Zn^{2+} ions, the side chain residues that coordinate the two metal centers and the bridging hydroxide group are shown as small spheres and sticks. L3 and L10 loops are highlighted with yellow shading. Note the limited flexibility of the L10 loop for the IMP-1 enzyme.

interactions with the ligand. For the IMP-1 enzyme, since there are no crystal structures in complex with cyclic boronate inhibitors as well as phosphates, it is unclear if a similar behavior might occur.

To get further insights into the induced-fit capacity of the catalytic center of B1 enzymes, the intrinsic shape-changing motions of these enzymes were analyzed by MD simulations. These enzyme motions are essential for the catalysis/inhibition (turnover) and are often modulated by ligand binding and might explain the experimentally observed selectivity of the cyclic boronate inhibitors against the B1 enzymes. These computational studies were performed on the unbound forms of IMP-1 and VIM-2 for 100 ns by using the enzyme coordinates of IMP-1 from *S. marcescens* (PDB 5EV6, 1.98 Å)[138] and VIM-2 from *P. aeruginosa* (PDB 5ACU, 2.10 Å)[146] (for further details see the Experimental Section). A truncated octahedron of water molecules obtained with the molecular mechanics force field AMBER was used to simulate the biological environment. The results of these simulations clearly showed that while the L3 loop (lid) is very flexible for both enzymes, for the L10 loop this is not the case (**Figure 10**). Thus, for the VIM-2 enzyme, the L10 loop proved to have large capacity to adopt ample and diverse arrangements to host ligands of different sizes, geometries, and conformational restrains. By contrast, for the IMP-1 enzyme, no significant motion of the L10 loop was observed during the whole simulation. Specifically, a large opening of the L3 and L10 loops of up to ≈8 and ≈10 Å, respectively, takes place for the VIM-2 enzyme, but for the IMP-1 enzyme only a significant opening of the L3 loop (≈10 Å) was observed. These clear differences and the limited plasticity of the L10 loop of the IMP-1 enzyme was also corroborated by examination of the vibrational modes calculated by principal-component analysis as implemented in AMBER (**Figure 11**).

Taken together, these findings suggested that the IMP-1 enzyme has reduced induced-fit capacity for binding conformational restricted ligands such as cyclic boronate inhibitors, which might explain the weak inhibition potency of vaborbactam and taniborbactam (micromolar) against this enzyme. In addition, the aforementioned structural differences, as well as dissimilar arrangement of the L3 loop between the three enzymes, would be responsible for the high affinity of taniborbactam for the VIM-1/2 and NDM-1 enzymes.

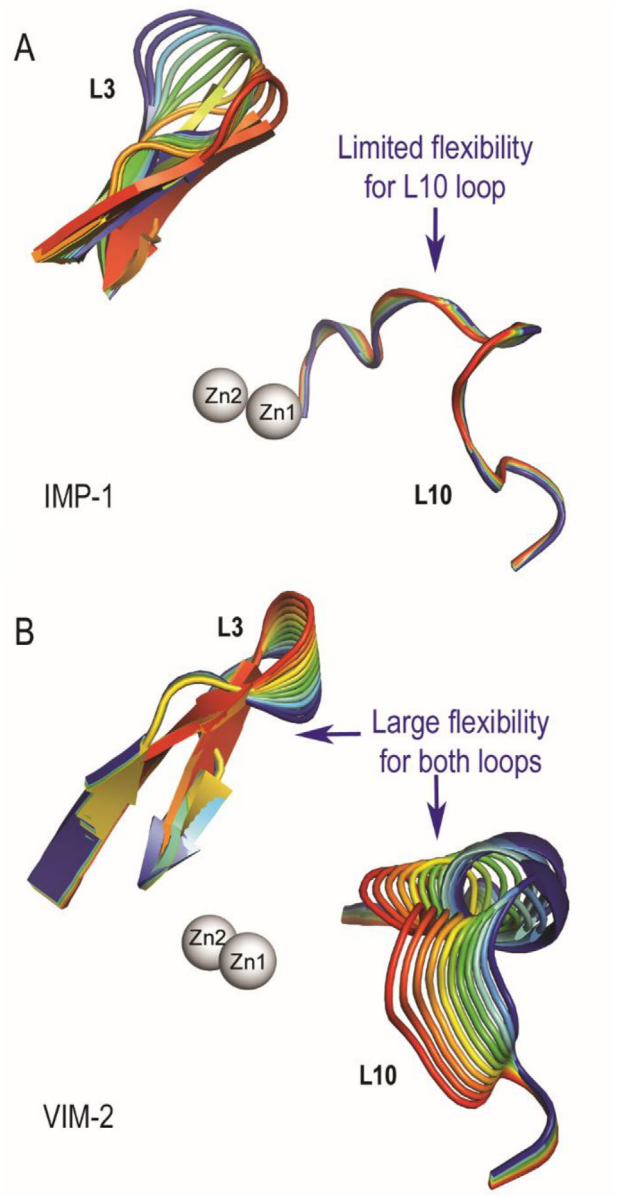

Figure 11. Overall view of the motion of the L3 and L10 loops of A) IMP-1 and B) VIM-2 obtained by examination of the vibrational modes. The main vibrational modes are presented.

5.2. QPX7728

Research efforts toward the development of ultrabroad-β-lactamase inhibitors have also been focused on exploring the effects of the substitution of the aromatic core of the 3,4-dihydro-2*H*-benzo[*e*][1,2]oxaborinin-2-ol scaffold. The *ortho* position to the carboxylate group has been the most widely studied.[147–150] The investigations carried out by researchers at Qpex Biopharma Inc. showed that this type of substitution is important for i) avoiding the formation of oligomers, which can be an issue at certain pHs and concentrations, and ii) reducing the impact of the MexAB-OprM efflux pump in bacterial strains of *P. aeruginosa*.[151] The types of substituents explored in the aromatic ring (R group) are summarized in **Figure 12** along with the two types of side chains (methylthioacetamide and 1,3,4-thiadiazolyl-2-thio groups) that provided the most relevant inhibitors. Among the substituents explored, small groups, such as methoxy and fluoro, provided the best results. The initial studies led to the identification of the methylthioacetamide derivative **24**, which unfortunately proved to inhibit only serine-β-lactamases of classes A and C. Subsequent studies allowed the identification of a more promising compound, bicyclic boronate **25**, that also proved to be active against class B enzymes. Compound **25** contains a 1,3,4-thiadiazolyl-2-thio-group in the α-position to the boron center and a methoxy group as a substituent on the aromatic core. Regretfully, as with taniborbactam, compounds **24** and **25** do not inhibit the worrisome carbapenemases of class D, such as OXA-23.

Surprisingly, the removal of the substituent in the α-position to the boron atom in the *ortho*-substituted derivative **25** provided an excellent ultrabroad-spectrum inhibitor, compound **26** (Figure 12B). Unlike derivative **25**, inhibitor **26** displays remarkable activity against the challenging carbapenemases of class D, specifically OXA-23 and OXA-72, which are widespread in *A. baumannii*.[147] In addition, compound **26** exhibits an improved activity profile against enzymes of classes A and C, and, as with compound **25**, retains excellent activity against the metallo-β-lactamases VIM-2 and NDM-1, but its activity against IMP-26 is worse than that of the parent compound. However, despite the excellent pharmacokinetic properties in rats, further development of compound **26** was discontinued because subsequent in vivo studies in dogs and monkeys revealed the formation of long-lived metabolites resulting from an oxidative deboronation process. Subsequent investigations aimed at avoiding the latter process by introducing small substituents in positions 3, 4 or both in **26** led to the discovery of QPX7728 (**3**), a metabolically stable, remarkably potent and ultrabroad-spectrum inhibitor with potential for both intravenous and oral application.[127,147,152] QPX7728 in combination with QPX2014 (chemical structure not yet disclosed) is currently under phase I clinical trials.

QPX7728 (**3**) is synthesized in ten steps from commercially available 2-bromo-5-fluorophenol (**27**) (**Scheme 2**).[148–150,153] Firstly, treatment of phenol **27** with Boc_2O and DMAP, followed by deprotonation of the resulting carbonate **28** by reaction with LDA to trigger the intramolecular migration of the vicinal carboxylate group, and reprotection of the resulting phenol gives compound **29**. Hydrolysis of the Boc and ester groups in **29** by treatment with TFA and subsequent intramolecular esterification by reaction with acetone in the presence of trific acid anhydride and TFA provide ester **30**. The required (*Z*)-vinylboronic acid pinanediolato ester moiety for the introduction of the cyclopropyl ring and formation of the bicyclic moiety in **3** is then achieved in three steps involving i) Heck cross-coupling between bromide **30** and acrylic acid, using $Pd(OAc)_2$ as catalyst and $P(o\text{Tol})_3$, ii) bromination of the resulting carboxylic acid **31** followed by decarboxylative elimination to afford the (*Z*)-bromovinyl derivative **32**; and iii) Suzuki cross-coupling between bromide **32** and bis[(+)-pinanediolato]diboron using $PdCl_2$(dppf) as catalyst. The palladium-catalyzed cyclopropanation of alkene **33** by treatment with diazomethane gives the two possible diastereoisomers **34** and **35**. Basic hydrolysis of the ester group and subsequent removal of the (+)-pinanediol lead to QPX7728 (**3**).

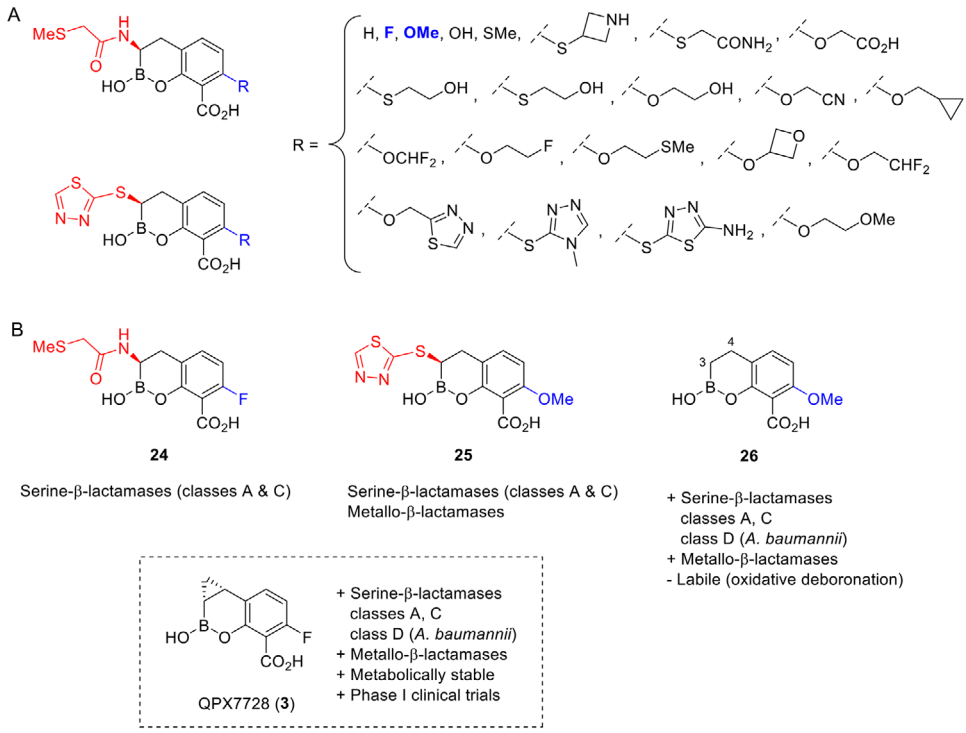

Figure 12. A) Examples of *ortho*-substituted bicyclic boronates explored. B) Chemical structures of the most relevant inhibitors identified and their scope of activity.

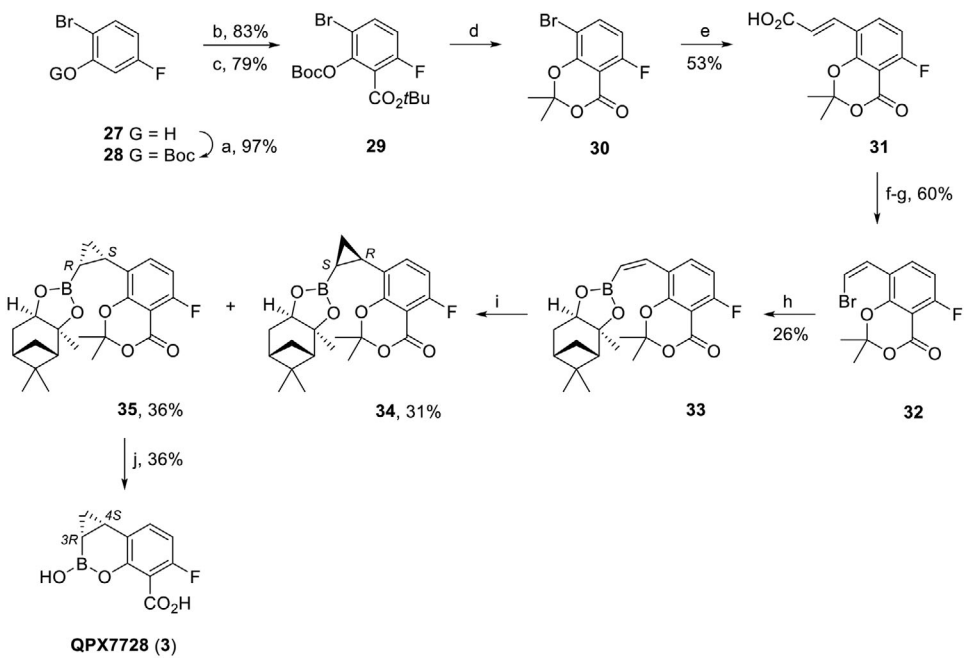

Scheme 2. Synthesis of QPX7728 (3). Reagents, and conditions: (a) Boc_2O, DMAP, CH_2Cl_2, RT. (b) LDA, THF, −78 °C to RT. (c) Boc_2O, DMAP, CH_2Cl_2, RT. (d) 1. TFA. 2. acetone, TFA, Tf_2O, 65 °C. (e) Acrylic acid, $Pd(OAc)_2$, $P(oTol)_3$, Et_3N, DMF, 100 °C. (f) Br_2, $CHCl_3$, 0 °C. (g) Et_3N, DMF, 0 °C. (h) bis[(+)-pinanediolato]diboron, $PdCl_2(dppf)$, KOAc, dioxane, 60 °C. (i) CH_2N_2, $Pd(OAc)_2$, THF, −10 °C to RT. (j) 1. NaOH (3 M), dioxane, RT. 2. Et_3SiH, TFA, $iBuB(OH)_2$, 0 °C.

Table 3. IC_{50} (nM) values of QPX7728 (**3**), vaborbactam (**4**), avibactam (**9**), and relebactam (**10**) against relevant serine- and metallo-β-lactamase enzymes.

Class	Enzyme	QPX7728 (**3**)[a,b]	Vaborbactam (**4**)[a,b]	Avibactam (**9**)[a,b]	Relebactam (**10**)[a,b]
A	TEM-10	2.2	470	4.3	160
	KPC-2	2.9	110	22	82
	SHV-12	1.9	56	0.61	330
	CTX-M-14	0.94	110	1.4	34
B1	IMP-1	610	>160 000	>160 000	>160 000
	NDM-1	55	>160 000	>160 000	>160 000
	VIM-1	14	>160 000	>160 000	>160 000
C	P99	22	88	26	36
D	OXA-23	1.2	120 000	3100	ND[c]
	OXA-48	1.1	6900	180	90 000

[a] IC_{50} values were measured using imipenem as substrate; [b] Data from ref. 154; [c] ND = not determined.

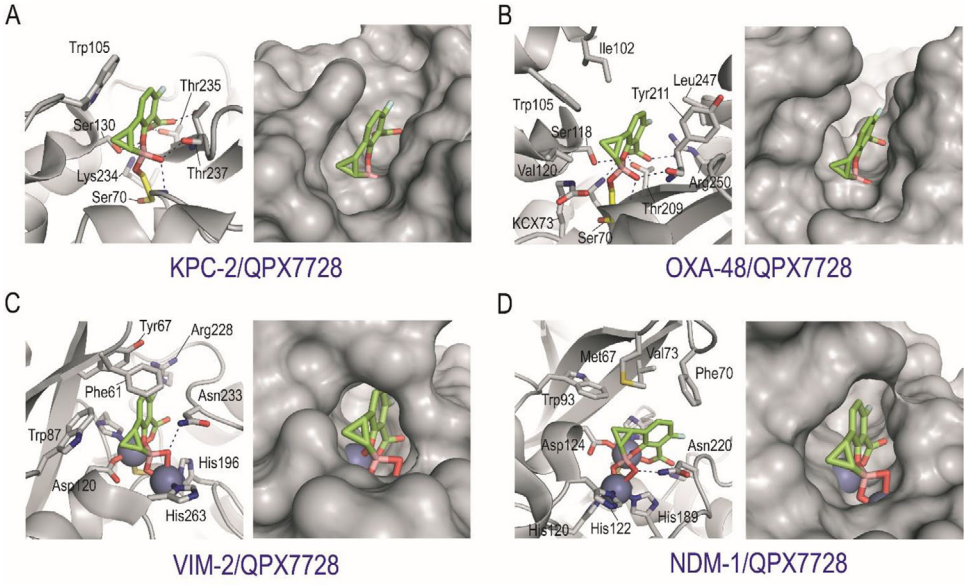

Figure 13. Crystal structures of serine- and metallo-β-lactamase enzymes in complex with QPX7728: A) KPC-2 from *K. pneumoniae* (PDB 6V1J[146]), B) OXA-48 from *K. pneumoniae* (PDB 6V1O[147]), C) VIM-2 from *P. aeruginosa* (PDB 6V1P[147]), and D) NDM-1 from *K. pneumoniae* (PDB 6V1M[147]). Relevant side chain residues are shown and labeled. Zn^{2+} ions are shown as spheres.

Biochemical assays showed that QPX7728 is a β-lactamase inhibitor with a groundbreaking spectrum of activity, including the most worrisome β-lactamases of the four classes. Thus, QPX7728 efficiently inhibits ESBLs, including class A carbapenemases such as KPC, as well as class C cephalosporinases such as P99, with IC_{50} values in the nanomolar range (**Table 3**).[154] The latter activity is comparable or better than those of other β-lactamase inhibitors in clinical use, such as avibactam, relebactam or vaborbactam. The most remarkable improvement for QPX7728 is against enzymes of metallo-β-lactamases and OXA-type enzymes. Thus, its inhibitory potency against class B enzymes, such as VIM-1 ($IC_{50} = 14 \times 10^{-9}$ M) and NDM-1 ($IC_{50} = 55 \times 10^{-9}$ M), as well as class D carbapenemases such as OXA-48 from *K. pneumoniae* ($IC_{50} = 1.1 \times 10^{-9}$ M) and OXA-23 from *A. baumannii* ($IC_{50} = 1.2 \times 10^{-9}$ M) is outstanding considering that the FDA approved inhibitors either show no significant activity (class B) or are up to 2500-fold less active (class D) against bacterial strains that express these hydrolases. QPX7728 is also better than durlobactam (phase III), which is efficient against OXA enzymes from *A. baumannii* but does not inhibit class B enzymes.[102,103] In general, the inhibitory profile of QPX7728 is also wider than the only clinically available boron-based inhibitor vaborbactam, which is a weak inhibitor of β-lactamases of classes B and D. Furthermore, its activity against OXA carbapenemases from *Acinetobacter* spp. is also an advantage over taniborbactam, the new boron-based inhibitor in phase III clinical trials.[131] On the other hand, QPX7728 does not inhibit mammalian serine and metalloproteases with the exception of cathepsin A, whose activity is currently being investigated further.

Microbiological studies with an extensive collection of bacterial strains have demonstrated the excellent capacity of QPX7728 to restore the antibiotic efficacy of diverse β-lactam antibiotics, either intravenously administered (ceftazidime, piperacillin,

cefepime, ceftolozane, meropenem), or orally bioavailable (ceftibuten, cefpodoxime, tebipenem).[153] Specifically, these studies were performed with strains that express ESBLs (CTX-M, SHV, TEM, VEB, PER), both plasmidic (CMY, FOX, MIR, DHA) and chromosomally encoded (P99, PDC, ADC) class C β-lactamases, class A carbapenemases (KPC, SME, NMC-A, BKC-1), class D carbapenemases (OXA-48, OXA-23, OXA-24/40, OXA-58), and class B carbapenemases (NDM, VIM, CcrA, IMP, and GIM). Moreover, susceptibility studies carried out on a large collection of carbapenem-resistant *Enterobacterales* revealed that the combination meropenem/QPX7728 has a very attractive microbiological profile for infections caused by pathogens with multiple resistance mechanisms.[155]

From the structural point of view, the main differences between taniborbactam (**1**) and QPX7728 (**3**) are i) the higher overall rigidity of the latter due to the additional restraint caused by the introduction of a cyclopropane ring in the 3,4-dihydro-2*H*-benzo[*e*][1,2]oxaborinin-2-ol scaffold, and ii) the extra and/or more potent contacts resulting from (a) the substitution with an electron-withdrawing group (fluoro), and (b) the incorporation of the cyclopropane moiety. Analysis of the available crystal structures of KPC-2 from *K. pneumoniae* (PDB 6V1J,[147] 1.3 Å), OXA-48 from *K. pneumoniae* (PDB 6V1O,[147] 1.8 Å), VIM-2 from *P. aeruginosa* (PDB 6V1P,[147] 1.2 Å), and NDM-1 from *K. pneumoniae* (PDB 6V1M,[147] 1.05 Å) in complex with QPX7728, revealed that option (ii) is more likely (**Figure 13**). Thus, in all of the structures the cyclopropane ring is located in an apolar pocket of the enzyme active site, and the aromatic ring is exquisitely flanked by residues that can establish CH–π interactions with this aromatic ring. The latter type of interaction is particularly relevant considering the electron-deficiency of this aromatic ring, which contains three electron-withdrawing substituents [F, CO_2, $OB(OH)_2$].[156] For instance, for the OXA-48/QPX7728 complex, the cyclopropyl moiety is surrounded by residues Trp105 and Val120, which are located close to the methylenic group, and the aromatic ring establishes CH–π interactions with the side chains of residues Tyr211, Ile102, and Leu247, which are flanking both faces of the ring. This arrangement explains the much weaker inhibitory potency of its enantiomer (3*S*,4*R*) (≈10-fold against OXA-type enzymes), particularly for those enzymes that have large apolar subpockets in the active site, such as OXA-48.[147]

6. Conclusion

The outstanding and ultrabroad-spectrum inhibitory capacity of taniborbactam, VNRX-7145, and QPX7728 against challenging β-lactamase enzymes, which have been summarized here, pinpoint bicyclic boronate inhibitors as the present hope against multidrug-resistant bacteria. With these recently discovered boron-based inhibitors a long-pursued unmet goal has been achieved, namely to restore the efficacy of β-lactam antibiotics against bacterial strains that produce metallo-β-lactamases, for which inhibitors in clinical use are not currently available. Even more relevant is the fact that these inhibitors open the door to the use of the same compound for therapies that involve bacterial strains that coproduce both serine- and metallo-β-lactamase enzymes. Although the great structural diversity of these types enzymes makes it challenging to find an excellent inhibitor for all of them, QPX7728 seems to be the most universal of the inhibitors produced to date. The future of this bicyclic boronate inhibitor, which is currently under phase I clinical studies in combination with QPX2014, looks exciting. It is important to ascertain whether future combinations of QPX7728 with β-lactam antibiotics in clinical use could enter clinical development. In any case, the excellent structural information available and the results already achieved augur well for a boom in research around the bicyclic boronate scaffold in the near future. One can envisage that this will eventually bring more effective therapeutic solutions for dealing with one of the most serious challenges in global health.

7. Computational Methods

Molecular Modeling Studies: All calculations were performed by using the Gaussian 09W[140] program package at DFT level by means of the B3LYP functional.[141,142] The standard 6–31+G(d,p)[143,144] basis set was used for C, H, O, S, B, and N, and the LANL2DZ relativistic pseudopotential was used for Zn.[145] The starting point of these calculations was taken from crystallographic structures PDB 6SP7 (chain E) including the following residues: Phe61, Trp87, His116, His118, Asp120, His196, CysS221, Gly232, Asn233, His263, both Zn atoms (labeled as residues 301 and 302), Zn-bonded taniborbactam (residue 306 named K9B) and the water molecule 441. All amino acids were truncated at Cα positions with a methyl group, except for Asn233, whose Cα was transformed into a methylene group keeping the nitrogen atom of the main chain and carbonyl group of Gly232 (transformed into an acetyl group). Hydrogen atoms were added to complete valences, considering all the histidine residues in the neutral form, and protonated in ϵ position except His118 protonated in δ position. Asp120 and Cys221 were used in the anionic form. The side chain of taniborbactam was truncated into an acetyl amide group, the oxygen atom O07 and the carboxylate group in the ligand were considered as hydroxyl and carboxylate groups, respectively. Vaborbactam was manually modeled from taniborbactam coordinates in a similar fashion. To represent better the geometry in the enzyme active site, minimization of both systems was performed while fixing the Cartesian coordinates for the Cα and Cβ atoms of all residues.

Molecular Dynamics Simulations Studies–Protein Preparation: The protein coordinates found in the crystal structure of IMP-1 from *S. marcescens* (PDB 5EV6, 1.98 Å)[138] and VIM-2 from *P. aeruginosa* (PDB 5ACU, 2.10 Å),[146] both in the wild-type form, were used. For the IMP-1 enzyme, coordinates from chain D were selected. Computation of the protonation state of all titratable groups at pH 7.0 was carried out using the H^{++} Web server.[157,158] As a result of this analysis His19 and His34 for IMP-1 and His55, His170, His252, His285, and His293 for VIM-2 were protonated in ϵ position. Parameterization of the Zn-contained active site was carried out as using MCPB module of AMBER Tools 17,[159,160] following the method described in the AMBER tutorial 2.4.[161] Active site of both enzymes consisted of the following residues: i) for coordination to Zn1 ion (residue number 301/1296): His77/His116, His79/His118, and His139/His196 (in IMP-1/VIM-2, respectively); ii) for coordination to Zn2 ion (residue number 302/1297): His197/His263, Asp81/Asp120, and Cys158/Cys221; and a water molecule (residue number 400/1001) situated between both Zn^{2+} cations that was modeled as hydroxide. All histidine residues were considered in their neutral form and coordinated to the Zn atoms through the nitrogen atom in ϵ position (NE2) except for His79/His118 that is coordinated through the nitrogen atom in δ position (ND1). Residues Asp81/Asp120 and Cys158/Cys221 both are bound in the anionic form through the atoms OD2 and SG, respectively.

The bond and angle force constants for the active site residues were determined from the sub matrices of the Cartesian Hessian matrix calculated using Gaussian 09 using the Seminario Method.[162] Partial charges for the active site residues were derived by quantum mechanical calculations using Gaussian 09, according to the RESP[163] model. Addition of hydrogen atoms and molecular mechanics parameters from the ff14SB[163] force field were assigned to the proteins using the LEaP

module of AMBER Tools 17. IMP-1 protein was immersed in a truncated octahedron of ≈9100 TIP3P water molecules and neutralized by addition of chloride ions. VIM-2 protein was immersed in a truncated octahedron of ≈6400 TIP3P water molecules and neutralized by addition of sodium ions.

Minimization of the Unbound Forms: The system was minimized in four stages: a) initial minimization of the active site residues, hydroxide and Zn ions (1000 steps, first half using steepest descent and the rest using conjugate gradient); b) minimization of the solvent and ions (5000 steps, first half using steepest descent and the rest using conjugate gradient); c) minimization of the side chain residues, waters, and ions (5000 steps, first half using steepest descent and the rest using conjugate gradient); d) final minimization of the whole system (5000 steps, first half using steepest descent, and the rest using conjugate gradient). A positional restraint force of 50 kcal mol^{-1} $Å^{-2}$ was applied to the whole system except the active site, the whole protein and α carbons during the first three stages (a–c), respectively.

Simulations of the Unbound Forms: MD simulations were performed using the pmemd.cuda_SPFP[165–167] module from the AMBER 16 suite of programs. Periodic boundary conditions were applied, and electrostatic interactions were treated using the smooth particle mesh Ewald method[168] with a grid spacing of 1 Å. The cutoff distance for the nonbonded interactions was 9 Å. The SHAKE algorithm[169] was applied to all bonds containing hydrogen using a tolerance of 10^{-5} Å and an integration step of 2.0 fs. The minimized system was then heated at 300 K at 1 atm by increasing the temperature from 0 to 300 K over 100 ps and by keeping the system at 300 K another 100 ps. A positional restraint force of 50 kcal mol^{-1} $Å^{-2}$ was applied to all α carbons during the heating stage. Finally, an equilibration of the system at constant volume (200 ps with positional restraints of 5 kcal mol^{-1} $Å^{-2}$ to α carbons) and constant pressure (another 100 ps with positional restraints of 5 kcal mol^{-1} $Å^{-2}$ to α carbons) was performed. The positional restraints were gradually reduced from 5 to 1 mol^{-1} $Å^{-2}$ (5 steps, 100 ps each), and the resulting systems were allowed to equilibrate further (100 ps) without restraints. Unrestrained MD simulations were carried out for 100 ns. System coordinates were collected every 10 ps for further analysis.

The molecular graphics program PyMOL[170] and CHIMERA[171] was employed for visualization and depicting enzyme structures. The cpptraj module in AMBER Tools 17 was used to analyze the trajectories and to calculate the rmsd of the protein during the simulation.[172] The vibrational modes for both metallo-β-lactamases were calculated by principal component analysis with the cpptraj module from the corresponding MD trajectories.[173]

Supporting Information

Supporting Information is available from the Wiley Online Library or from the author.

Acknowledgements

Financial support from the Spanish Ministry of Economy and Competeness (SAF2016-75638-R, PID2019-105512RB-I00), the Xunta de Galicia [ED431B 2018/04 and Centro singular de investigación de Galicia accreditation 2019–2022 (ED431G 2019/03)], and the European Regional Development Fund (ERDF) is gratefully acknowledged. The authors also thank the Centro de Supercomputación de Galicia (CESGA) for use of the Finis Terrae computer.

Conflict of Interest

The authors declare no conflict of interest.

Keywords

antibiotic adjuvants, boron-based inhibitors, metallo-β-lactamases, resistance breakers, serine-β-lactamases

Received: October 30, 2020
Revised: December 6, 2020
Published online: February 15, 2021

[1] A. M. Thayer, *Chem. Eng. News* **2016**, *94*, 36.
[2] E. D. Brown, G. D. Wright, *Nature* **2016**, *529*, 336.
[3] C. L. Ventola, *Pharm. Ther.* **2015**, *40*, 277.
[4] I. Levin-Reisman, I. Ronin, O. Gefen, I. Braniss, N. Shoresh, N. Q. Balaban, *Science* **2017**, *355*, 826.
[5] M. E. A. de Kraker, A. J. Stewardson, S. Harbarth, *PLoS Med.* **2016**, *13*, 1002184.
[6] N. Gilbert, *Nature* **2018**, *555*, S5.
[7] C. Lepore, L. Silver, U. Theuretzbacher, J. Thomas, D. Visi, *Nat. Rev. Drug Discovery* **2019**, *18*, 739.
[8] S. Chakradhar, *Nat. Med.* **2016**, *22*, 1197.
[9] C. González-Bello, *Bioorg. Med. Chem. Lett.* **2017**, *27*, 4221.
[10] E. E. Gill, O. L. Franco, R. E. W. Hancock, *Chem. Biol. Drug Des.* **2015**, *85*, 56.
[11] P. Bernal, C. Molina-Santiago, A. Daddaoua, M. A. Llamas, *Microb. Biotechnol.* **2013**, *6*, 445.
[12] H. Douafer, V. Andrieu, O. Phanstiel, J. M. Brunel, *J. Med. Chem.* **2019**, *62*, 8665.
[13] M. A. Farha, E. D. Brown, *Nat. Biotechol.* **2013**, *31*, 120.
[14] D. Brown, *Nat. Rev. Drug Discovery* **2015**, *14*, 821.
[15] R. J. Worthington, C. Melander, *Trends Biotechnol.* **2013**, *31*, 177.
[16] G. D. Wright, *Trends Microb.* **2016**, *24*, 862.
[17] K. Bush, *ACS Infect. Dis.* **2015**, *13*, 509.
[18] R. I. Melander, C. Melander, *ACS Infect. Dis.* **2017**, *3*, 559.
[19] L. Kalan, G. D. Wright, *Expert Rev. Mol. Med.* **2011**, *13*, 5.
[20] J. A. Hill, L. E. Cowen, *Future Microbiol.* **2015**, *10*, 1719.
[21] K. Bush, P. A. Bradford, *Cold Spring Harb. Perspect. Med.* **2016**, *6*, 025247.
[22] M. Toth M, N. T. Antunes, N. K. Stewart, H. Frase, M. Bhattacharya, C. A. Smith, S. B. Vakulenko, *Nat. Chem. Biol.* **2016**, *12*, 9.
[23] K. Poole, *Cell Mol. Life Sci.* **2004**, *61*, 2200.
[24] R. P. Elander, *Appl. Microbiol. Biotechnol.* **2003**, *61*, 385.
[25] C. Walsh, *Nature* **2000**, *406*, 775.
[26] C. L. Tooke, P. Hinchi, E. C. Bragginton, C. K. Colenso, V. H. A. Hirvonen, Y. Takebayashi, J. Spencer, *J. Mol. Biol.* **2019**, *431*, 3472.
[27] K. Baren, P. A. Bradford, *Clin. Microbiol. Rev.* **2020**, *33*, e00047-19.
[28] WHO, Global priority list of antibiotic-resistant bacteria to guide research, discovery, and development of new antibiotics, http://www.who.int/medicines/publications/WHO-PPL-Short_Summary_25Feb-ET_NM_WHO.pdf?ua=1 (accessed: July **2020**).
[29] T. Naas, S. Oueslati, R. A. Bonnin, M. L. Dabos, A. Zavala, L. Dortet, P. Retailleau, B. I. Iorga, *J. Enzyme Inhib. Med. Chem.* **2017**, *32*, 917.
[30] K. Bush, P. A. Bradford, *Nat. Rev. Microbiol.* **2019**, *17*, 295.
[31] K. Bush, *Antimicrob. Agents Chemother.* **2018**, *62*, e01076-18.
[32] K. Bush, *Ann. N. Y. Acad. Sci.* **2013**, *1277*, 84.
[33] C. González-Bello, D. Rodríguez, M. Pernas, A. Rodríguez, E. Colchón, *J. Med. Chem.* **2020**, *63*, 1859.
[34] A. Krajnc, P. A. Lang, T. D. Panduwawala, J. Brem, C. J. Schofield, *Curr. Opin. Chem. Biol.* **2019**, *50*, 101.
[35] A. Philippon, P. Slama, P. Dény, R. Labia, *Clin. Microbiol. Rev.* **2016**, *29*, 29.
[36] J. Walther-Rasmussen, N. Høiby, *J. Antimicrob. Chemother.* **2007**, *60*, 470.
[37] G. A. Jacoby, *Clin. Microbiol. Rev.* **2009**, *22*, 161.
[38] C. Juan, G. Torrens, M. González-Nicolau, A. Oliver, *FEMS Microbiol. Rev.* **2017**, *41*, 781.
[39] D. A. Leonard, R. A. Bonomo, R. A. Powers, *Acc. Chem. Res.* **2013**, *46*, 2407.

[40] K.-C. J. Kaitany, N. V. Klinger, C. M. June, M. E. Ramey, R. A. Bonomo, R. A. Powers, D. A. Leonard, *Antimicrob. Agents Chemother.* **2013**, *57*, 4848.
[41] L. Poirel, T. Naas, P. Nordmann, *Antimicrob. Agents Chemother.* **2010**, *54*, 24.
[42] B. A. Evans, S. G. Amyes, *Clin. Microbiol. Rev.* **2014**, *27*, 241.
[43] M. Afzal-Shah, N. Woodford, D. M. Livermore, *Antimicrob. Agents Chemother.* **2001**, *45*, 583.
[44] A. M. Queenan, K. Bush, *Clin. Microbiol. Rev.* **2007**, *20*, 440.
[45] G. Bou, A. Oliver, J. Martínez-Beltrán, *Antimicrob. Agents Chemother.* **2000**, *44*, 1556.
[46] S. Corvec, L. Poirel, T. Naas, H. Drugeon, P. Nordmann, *Antimicrob. Agents Chemother.* **2007**, *51*, 1530.
[47] L. Poirel, S. Marqué, C. Héritier, C. Segonds, G. Chabanon, P. Nordmann, *Antimicrob. Agents Chemother.* **2005**, *49*, 202.
[48] T. Palzkill, *Ann. N. Y. Acad. Sci.* **2013**, *1277*, 91.
[49] P. Linciano, L. Cendron, E. Gianquinto, F. Spyrakis, D. Tondi, *ACS Infect. Dis.* **2019**, *5*, 9.
[50] P. Salahuddin, A. Kumar, A. U. Khan, *Curr. Protein Pept. Sci.* **2018**, *19*, 130.
[51] I. Garcia-Saez, J. D. Docquier, G. M. Rossolini, O. Dideberg, *J. Mol. Biol.* **2008**, *375*, 604.
[52] H. Park, E. N. Brothers, K. M. Merz, *J. Am. Chem. Soc.* **2005**, *127*, 4232.
[53] A. I. Karsisiotis, C. F. Damblon, G. C. K. Roberts, *Metallomics* **2014**, *6*, 1181.
[54] H. Zhang, Q. Hao, *FASEB J.* **2011**, *25*, 2574.
[55] D. T. King, L. J. Worrall, R. Gruninger, N. C. Strynadka, *J. Am. Chem. Soc.* **2012**, *134*, 11362.
[56] M. R. Meini, L. I. Llarrull, A. J. Vila, *FEBS Lett.* **2015**, *589*, 3419.
[57] M.-N. Lisa, A. R. Palacios, M. Aitha, M. M. González, D. M. Moreno, M. W. Crowder, R. A. Bonomo, J. Spencer, D. L. Tierney, L. I. Llarrull, A. J. Vila, *Nat. Commun.* **2017**, *8*, 538.
[58] H. Feng, X. Liu, S. Wang, J. Fleming, D.-C. Wang, W. Liu, *Nat. Commun.* **2017**, *8*, 2242.
[59] A. U. Khan, L. Maryam, R. Zarrilli, *BCM Microbiol.* **2017**, *17*, 101.
[60] P. Nordmann, L. Dortet, L. Poirel, *Trends Mol. Med.* **2012**, *18*, 263.
[61] C. Bebrone, *Biochem. Pharmacol.* **2007**, *74*, 1686.
[62] G. Garau, C. Bebrone, C. Anne, M. Galleni, J. M. Frère, O. Dideberg, *J. Mol. Biol.* **2005**, *345*, 785.
[63] C. Bebrone, H. Delbrück, M. B. Kupper, P. Schlömer, C. Willmann, J. M. Frère, R. Fischer, M. Galleni, K. M. Hoffmann, *Antimicrob. Agents Chemother.* **2009**, *53*, 4464.
[64] R. P. McGeary, D. T. Tan, G. Schenk, *Future Med. Chem.* **2017**, *9*, 673.
[65] M. P. Pedroso, D. W. Waite, O. Melse, L. Wilson, N. Mitic, R. P. McGeary, I. Antes, L. W. Guddat, P. Hugenholtz, G. Schenk, *Protein Cell* **2020**, *11*, 613.
[66] Z. Cheng, C. A. Thomas, A. R. Joyner, R. L. Kimble, A. M. Sturgill, N. Y. Tran, M. R. Vulcan, S. A. Klinsky, D. J. Orea, C. R. Platt, F. Cao, B. Li, Q. Yang, C. J. Yurkiewicz, W. Fast, M. W. Crowder, *Biomolecules* **2020**, *10*, 459.
[67] H. J. Morrill, J. M. Pogue, K. S. Kaye, K. L. LaPlante, *Open Forum Infect. Dis.* **2015**, *2*, 050.
[68] R. F. Potter, A. W. D'Souza, G. Dantas, *Drug Resist. Updat.* **2016**, *29*, 30.
[69] D. van Duin, Y. Doi, *Virulence* **2017**, *8*, 460.
[70] P. Nordmann, L. Poirel, *Clin. Infect. Dis.* **2019**, *69*, S521.
[71] M. I. Abboud, C. Damblon, J. Brem, N. Smargiasso, P. Mercuri, B. Gilbert, A. M. Rydzik, T. D. W. Claridge, C. J. Schofield, J.-M. Frère, *Antimicrob. Agents Chemother.* **2016**, *60*, 5655.
[72] C. Lascols, M. Hackel, S. H. Marshall, A. M. Hujer, S. Bouchillon, R. Badal, D. Hoban, R. A. Bonomo, *J. Antimicrob. Chemother.* **2011**, *66*, 1992.
[73] F. Al-Marzooq, Y. F. Ngeow, S. T. Tay, *Int. J. Antimicrob. Agents* **2015**, *45*, 445.
[74] S. N. Seiffert, J. Marschall, V. Perreten, A. Carattoli, H. Furrer, A. Endimiani, *Int. J. Antimicrob. Agents* **2014**, *44*, 260.
[75] M. Avolio, C. Vignaroli, M. Crapis, A. Camporese, *Future Microbiol.* **2017**, *12*, 1119.
[76] T. Kwon, J. W. Yang, S. Lee, M. R. Yun, W. G. Yoo, H. S. Kim, J. O. Cha, D. W. Kim, *Genome Announc.* **2016**, *4*, e01550-15.
[77] C. A. Moubareck, S. F. Mouftah, T. Pal, A. Ghazawi, D. H. Halat, A. Nabi, M. A. AlSharhan, Z. O. AlDeesi, C. C. Peters, H. Celiloglu, M. Sannegowda, D. K. Sarkis, A. Sonnevend, *Int. J. Antimicrob. Agents* **2018**, *52*, 90.
[78] T. Tada, T. Miyoshi-Akiyama, R. K. Dahal, S. K. Mishra, H. Ohara, K. Shimada, T. Kirikae, B. M. Pokhrel, *Int. J. Antimicrob. Agents* **2013**, *42*, 372.
[79] D. A. Contreras, S. P. Fitzwater, D. D. Nanayakkara, J. Schaenman, G. M. Aldrovandi, O. B. Garner, S. Yang, *Antimicrob. Agents Chemother.* **2020**, *64*, e00948-19.
[80] D. R. Giacobbe, M. Bassetti, F. G. De Rosa, V. del Bono, P. A. Grossi, F. Menichetti, F. Pea, G. M. Rossolini, M. Tumbarello, P. Viale, C. Viscoli, ISGRI-SITA (Italian Study Group on Resistant Infections of the Società Italiana Terapia Antinfettiva), *Expert Rev. Anti-Infect. Ther.* **2018**, *16*, 307.
[81] B. D. VanScoy, D. Tenero, S. Turner, D. M. Livermore, J. McCauley, H. Conde, S. M. Bhavnani, C. M. Rubino, P. G. Ambrose, *Antimicrob. Agents Chemother.* **2017**, *61*, e01052-17.
[82] L. Tselepis, G. W. Langley, A. F. Aboklaish, E. Widlake, D. E. Jackson, T. R. Walsh, C. J. Schofield, J. Brem, J. M. Tyrrell, *Int. J. Antimicrob. Agents* **2020**, *56*, 105925.
[83] A. Bonnefoy, C. Dupuis-Hamelin, V. Steier, C. Delachaume, C. Seys, T. Stachyra, M. Fairley, M. Guitton, M. Lampilas, *J. Antimicrob. Chemother.* **2004**, *54*, 410.
[84] K. Garber, *Nat. Rev. Drug Discovery* **2015**, *14*, 445.
[85] A. Vena, N. Castaldo, M. Bassetti, *Curr. Opin. Infect. Dis.* **2019**, *32*, 638.
[86] K. L. Chew, M. K. L. Tay, B. Cheng, R. T. P. Lin, S. Octavia, J. W. P. Teo, *Antimicrob. Agents Chemother.* **2018**, *62*, e00414-18.
[87] J. A. Karlowsky, K. M. Kazmierczak, B. L. M. de Jonge, M. A. Hackel, D. F. Sahm, P. A. Bradford, *Antimicrob. Agents Chemother.* **2017**, *61*, e00472-17.
[88] C. Ramsey, A. P. MacGowan, *J. Antimicrob. Chemother.* **2016**, *71*, 2704.
[89] M. A. Powles, A. Galgoci, A. Misura, L. Colwell, K. H. Dingley, W. Tang, J. Wu, T. Blizzard, M. Motyl, K. Young, *Antimicrob. Agents Chemother.* **2018**, *62*, e02577-17.
[90] J. Wu, F. Racine, M. K. Wismer, K. Young, D. M. Carr, J. C. Xiao, R. Katwaru, Q. Si, P. Harradine, M. Motyl, P. R. Bhagunde, M. L. Rizk, *Antimicrob. Agents Chemother.* **2018**, *62*, e02323-17.
[91] D. M. Livermore, S. Mushtaq, M. Warner, A. Vickers, N. Woodford, *J. Antimicrob. Chemother.* **2017**, *72*, 1373.
[92] Z. Khan, A. Iregui, D. Landman, J. Quale, *J. Antimicrob. Chemother.* **2019**, *74*, 2938.
[93] A. J. Lepak, M. Zhao, D. R. Andes, *Antimicrob. Agents Chemother.* **2019**, *63*, e01648-19.
[94] S. Mushtaq, A. Vickers, N. Woodford, A. Haldimann, D. M. Livermore, *J. Antimicrob. Chemother.* **2019**, *74*, 953.
[95] T. E. Asempa, A. Motos, K. Abdelraouf, C. Bissantz, C. Zampaloni, D. P. Nicolau, *Int. J. Antimicrob. Chemother.* **2020**, *55*, 105838.
[96] M. D. Barnes, M. A. Taracila, C. E. Good, S. Bajaksouzian, R. J. Rojas, D. van Duin, B. N. Kreiswirth, M. R. Jacobs, A. Haldimann, K. M. Papp-Wallace, R. A. Bonomo, *Antimicrob. Agents Chemother.* **2019**, *63*, e00432-19.
[97] B. Moya, I. M. Barcelo, S. Bhagwat, M. Patel, G. Bou, K. M. Papp-Wallace, R. A. Bonomo, A. Oliver, *Antimicrob. Agents Chemother.* **2017**, *61*, e01238-17.

[98] N. L. Mallalieu, E. Winter, S. Fettner, K. Patel, E. Zwanziger, G. Attley, I. Rodriguez, A. Kano, S. M. Salama, D. Bentley, A. M. Geretti, *Antimicrob. Agents Chemother.* **2020**, *64*, e02229-19.
[99] S. D. Lahiri, S. Mangani, H. Jahic, M. Benvenuti, T. F. Durand-Reville, F. De Luca, D. E. Ehmann, G. M. Rossolini, R. A. Alm, J. D. Docquier, *ACS Chem. Biol.* **2015**, *10*, 591.
[100] T. F. Durand-Réville, S. Gluler, J. Comita-Prevoir, B. Chen, N. Bifulco, H. Huynh, S. Lahiri, A. B. Shapiro, S. M. McLeod, N. M. Carter, S. H. Moussa, C. Velez-Vega, N. B. Olivier, R. McLaughlin, N. Gao, J. Thresher, T. Palmer, B. Andrews, R. A. Giacobbe, J. V. Newman, D. E. Ehmann, B. de Jonge, J. O´Donnell, J. P. Mueller, R. A. Tommasi, A. A. Miller, *Nat. Microbiol.* **2017**, *2*, 17104.
[101] O. Sagan, R. Yakubsevitch, K. Yanev, R. Fomkin, E. Stone, D. Hines, J. O'Donnell, A. Miller, R. Isaacs, S. Srinivasan, *Antimicrob. Agents Chemother.* **2020**, *64*, e01506-19.
[102] M. D. Barnes, V. Kumar, C. R. Bethel, S. H. Moussa, J. O'Donnell, J. D. Rutter, C. E. Good, K. M. Hujer, A. M. Hujer, S. H. Marshall, B. N. Kreiswirth, S. S. Richter, P. N. Rather, M. R. Jacobs, K. M. Papp-Wallace, F. van den Akker, R. A. Bonomo, *mBio* **2019**, *10*, e00159-19.
[103] T. F. Durand-Reville, J. Comita-Prevoir, J. Zhang, X. Wu, T. May-Dracka, J. Romero, F. Wu, A. Chen, A. B. Shapiro, N. Carter, S. McLeod, R. Giacobbe, J. Verheijen, S. Lahiri, M. Sacco, Y. Chen, J. O'Donnell, A. A. Miller, J. P. Mueller, R. Tommasi, *J. Med. Chem.* **2020**, *63*, 12511.
[104] J. O'Donnell, A. Tanudra, A. Chen, D. Hines, R. Tommasi, J. Mueller, *ACS Infect. Dis.* **2020**, *6*, 1378.
[105] A. A. Miller, A. B. Shapiro, S. M. McLeod, N. M. Carter, S. H. Moussa, R. Tommasi, J. P. Mueller, *ACS Infect. Dis.* **2020**, *6*, 1389.
[106] A. G. Stewart, P. N. A. Harris, A. Henderson, M. A. Schembri, D. L. Paterson, *J. Antimicrob. Chemother.* **2020**, *75*, 2384.
[107] J. Plescia, N. Moitessie, *Eur. J. Med. Chem.* **2020**, *195*, 112270.
[108] R. C. Kane, A. T. Farrell, R. Sridhara, R. Pazdur, *Clin. Cancer Res.* **2006**, *12*, 2955.
[109] M. Shirley, *Drugs* **2016**, *76*, 405.
[110] A. Markham, *Drugs* **2014**, *74*, 1555.
[111] O. Dobozy, I. Mile, I. Ferencz, V. Csányi, *Acta Biochim. Biophys. Acad. Sci. Hung.* **1971**, *6*, 97.
[112] R. Martin, J. B. Jones, *Tetrahedron Lett.* **1995**, *36*, 8399.
[113] D. Tondi, R. A. Powers, E. Caselli, M. C. Negri, J. Blázquez, M. P. Costi, B. K. Shoichet, *Chem. Biol.* **2001**, *8*, 593.
[114] C. T. Lohans, D. W. Wareham, H. P. Oswin, J. Mohammed, J. Spencer, C. W. Fishwick, M. A. McDonough, C. J. Schofield, J. Brem, *Antimicrob. Agents Chemother.* **2017**, *61*, e02260-16.
[115] S. T. Cahill, J. M. Tyrrell, I. H. Navratilova, K. Calvopiña, S. W. Robinson, C. T. Lohans, M. A. McDonough, R. Cain, C. W. G. Fishwick, M. B. Avison, T. R. Walsh, C. J. Schofield, J. Brem, *Biochim. Biophys. Acta, Gen. Subj.* **2019**, *1863*, 742.
[116] S. J. Baker, C. Z. Ding, T. Akama, Y.-K. Zhang, V. Hernandez, Y. Xia, *Future Med. Chem.* **2009**, *1*, 1275.
[117] S. Ness, R. Martin, A. M. Kindler, M. Paetzel, M. Gold, S. E. Jensen, J. B. Jones, N. C. Strynadka, *Biochemistry* **2000**, *39*, 5312.
[118] C. J. Burns, R. Goswami, R. W. Jackson, T. Lessen, W. Li, D. C. Pevear, P. K. Tirunahari, H. Xu, (Protez pharmaceuticals, Inc), *WO 2010/130708A1*, **2010**.
[119] C. J. Burns, D. Daigle, B. Liu, D. McGrarry, D. C. Pevear, R. E. L. Trout, (Protez pharmaceuticals, Inc), *WO 2014/089365A1*, **2014**.
[120] C. J. Burns, D. Daigle, B. Liu, R. W. Jackson, J. Hamrick, D. McGrarry, D. C. Pevear, R. E. L. Trout, (Protez pharmaceuticals, Inc), *WO 2015/191907A1*, **2015**.
[121] C. J. Burns, D. Daigle, B. Liu, D. McGrarry, D. C. Pevear, E. L. Trout, (Venatorx pharmaceuticals, Inc), *WO 2014/151958A1*, **2014**.
[122] C. J. Burns, D. Daigle, B. Liu, D. McGrarry, D. C. Pevear, E. L. Trout, R. W. Jackson, (Venatorx pharmaceuticals, Inc), *US 2014/0194386*, **2014**.
[123] S. J. Hecker, K. R. Reddy, M. Totrov, G. C. Hirst, O. Lomovskaya, D. C. Griffith, P. King, R. Tsivkovski, D. Sun, M. Sabet, Z. Tarazi, M. C. Clifton, K. Atkins, A. Raymond, K. T. Potts, J. Abendroth, S. H. Boyer, J. S. Loutit, E. E. Morgan, S. Durso, M. N. Dudley, *J. Med. Chem.* **2015**, *58*, 3682.
[124] G. Hirst, R. Reddy, S. Hecker, M. Totrov, D. C. Griffith, O. Rodny, M. N. Dudley, S. Boyer, (Rempex Pharmaceuticals, Inc), *WO2012/021455A1*, **2012**.
[125] S. Dhillon, *Drugs* **2018**, *78*, 1259.
[126] C. L. Tooke, P. Hinchliffe, A. Krajnc, A. J. Mulholland, J. Brem, C. J. Schofield, J. Spencer, *RSC Med. Chem.* **2020**, *11*, 491.
[127] R. Tsivkovski, O. Lomovskaya, *Antimicrob. Agents Chemother.* **2020**, *64*, e01935-19.
[128] G. W. Langley, R. Cain, J. M. Tyrrell, P. Hinchliffe, K. Calvopiña, C. L. Tooke, E. Widlake, C. G. Dowson, J. Spencer, T. R. Walsh, C. J. Schofield, J. Brem, *Bioorg. Med. Chem. Lett.* **2019**, *29*, 1981.
[129] J. C. Hamrick, J.-D. Docquier, T. Uehara, C. L. Myers, D. A. Six, C. L. Chatwin, K. J. John, S. F. Vernacchio, S. M. Cusick, R. E. L. Trout, C. Pozzi, F. De Luca, M. Benvenuti, S. Mangani, B. Liu, R. W. Jackson, G. Moeck, L. Xerri, C. J. Burns, D. C. Pevear, D. M. Daigle, *Antimicrob. Agents Chemother.* **2020**, *64*, e01963-19.
[130] A. Krajnc, J. Brem, P. Hinchliffe, K. Calvopina, T. D. Panduwawala, P. A. Lang, J. J. A. G. Kamps, J. M. Tyrrell, E. Widlake, B. G. Saward, T. R. Walsh, J. Spencer, C. J. Schofield, *J. Med. Chem.* **2019**, *62*, 8544.
[131] B. Liu, R. E. L. Trout, G.-H. Chu, D. McGarry, R. W. Jackson, J. C. Hamrick, D. M. Daigle, S. M. Cusick, C. Pozzi, F. De Luca, M. Benvenuti, S. Mangani, J.-D. Docquier, W. J. Weiss, D. C. Pevear, L. Xerri, C. J. Burns, *J. Med. Chem.* **2020**, *63*, 2789.
[132] S. Mushtaq, A. Vickers, M. Doumith, M. J. Ellington, N. Woodford, D. M. Livermore, *J. Antimicrob. Chemother.* **2021**, *76*, 160.
[133] C. J. Burns, R. Trout, A. Zulli, E. Mesaros, R. Jackson, S. Boyd, B. Liu, L. McLaughlin, C. Chatwin, J. Hamrick, D. Daigle, D. Pevear, *257th National Meet. Exposition of the American Chemical Society, Orlando, FL, U.S., March 31–April 4, 2019*, American Chemical Society, Washington, DC **2019**.
[134] J. Hamrick, C. Chatwin, K. John, C. Burns, L. Xerri, G. Moeck, D. Pevear, *29th ECCMID, Amsterdam, The Netherlands, April 13–16, 2019*, European Society of Clinical Microbiology and Infectious Diseases, Switzerland **2019**.
[135] L. M. Salonen, M. Ellermann, F. Diederich, *Angew. Chem., Int. Ed.* **2011**, *50*, 4808.
[136] A. Cardomí, J. C. Gómez-Tamayo, V. Gigoux, D. Fourmy, *Trends Pharmacol. Sci.* **2013**, *34*, 320.
[137] M. Maneiro, A. Peón, E. Lence, J. M. Otero, M. J. van Raaij, P. Thompson, A. R. Hawkins, C. González-Bello, *Biochem. J.* **2014**, *462*, 415.
[138] P. Hinchliffe, M. M. González, M. F. Mojica, J. M. González, V. Castillo, C. Saiz, M. Kosmopoulou, C. L. Tooke, L. I. Llarrull, G. Mahler, R. A. Bonomo, A. J. Vila, J. Spencer, *Proc. Natl. Acad. Sci. USA* **2016**, *113*, E3745.
[139] M. Aitha, A. R. Marts, A. Bergstrom, A. J. Møller, L. Moritz, L. Turner, J. C. Nix, R. A. Bonomo, R. C. Page, D. L. Tierney, M. W. Crowder, *Biochemistry* **2014**, *53*, 7321.
[140] M. J. Frisch, G. W. Trucks, H. B. Schlegel, G. E. Scuseria, M. A. Robb, J. R. Cheeseman, G. Scalmani, V. Barone, G. A. Petersson, H. Nakatsuji, X. Li, M. Caricato, A. Marenich, J. Bloino, B. G. Janesko, R. Gomperts, B. Mennucci, H. P. Hratchian, J. V. Ortiz, A. F. Izmaylov, J. L. Sonnenberg, D. Williams-Young, F. Ding, F. Lipparini, F. Egidi, J. Goings, B. Peng, A. Petrone, T. Henderson, D. Ranasinghe, V. G. Zakrzewski, J. Gao, N. Rega, G. Zheng, W. Liang, M. Hada, M. Ehara, K. Toyota, R. Fukuda, J. Hasegawa, M. Ishida, T. Nakajima, Y. Honda, O. Kitao, H. Nakai, T. Vreven, K. Throssell, J. A. Montgomery, Jr., J. E. Peralta, F. Ogliaro, M. Bearpark, J. J. Heyd, E. Brothers, K. N. Kudin, V. N. Staroverov, T. Keith, R. Kobayashi,

J. Normand, K. Raghavachari, A. Rendell, J. C. Burant, S. S. Iyengar, J. Tomasi, M. Cossi, J. M. Millam, M. Klene, C. Adamo, R. Cammi, J. W. Ochterski, R. L. Martin, K. Morokuma, O. Farkas, J. B. Foresman, D. J. Fox, Gaussian 09, Revision E.01, Wallingford, CT, **2016**.
[141] A. D. Becke, *J. Chem. Phys.* **1993**, *98*, 5648.
[142] P. J. Stephens, F. J. Devlin, C. F. Chabalowski, M. J. Frisch, *J. Phys. Chem.* **1994**, *98*, 11623.
[143] G. A. Petersson, A. Bennett, T. G. Tensfeldt, M. A. Al-Laham, W. A. Shirley, J. Mantzaris, *J. Chem. Phys.* **1988**, *89*, 2193.
[144] G. A. Petersson, M. A. Al-Laham, *J. Chem. Phys.* **1991**, *94*, 6081.
[145] G. A. Petersson, A. Bennett, T. G. Tensfeldt, M. A. Al-Laham, W. A. Shirley, J. Mantzaris, *J. Chem. Phys.* **1988**, *89*, 2193.
[146] T. Christopeit, T. J. O. Carlsen, R. Helland, H.-K. S. Leiros, *J. Med. Chem.* **2015**, *58*, 8671.
[147] S. J. Hecker, K. R. Reddy, O. Lomovskaya, D. C. Griffith, D. Rubio-Aparicio, K. Nelson, R. Tsivkovski, D. Sun, M. Sabet, Z. Tarazi, J. Parkinson, M. Totrov, S. H. Boyer, T. W. Glinka, O. A. Pemberton, Y. Chen, M. N. Dudley, *J. Med. Chem.* **2020**, *63*, 7491.
[148] R. Reddy, T. Glinka, M. Totrov, S. Hecker, (Rempex Pharmaceuticals, Inc.), *WO 2014/107535A1*, **2014**.
[149] R. Reddy, T. Glinka, S. Hecker, M. Totrov, O. Rodny, (Rempex pharmaceuticals, Inc), *WO 2015/179308A1*, **2015**.
[150] R. K. Reddy, T. Glinka, M. Totrov, S. Hecker, O. Rodny, (Rempex pharmaceuticals, Inc), *WO 2016/003929A1*, **2016**.
[151] O. Lomovskaya, K. Nelson, D. Rubio-Aparicio, R. Tsivkovski, D. Sun, M. N. Dudley, *Antimicrob. Agents Chemother.* **2020**, *64*, e00552-20.
[152] O. Lomovskaya, R. Tsivkovski, K. Nelson, D. Rubio-Aparicio, D. Sun, M. Totrov, M. N. Dudley, *Antimicrob. Agents Chemother.* **2020**, *64*, e00212-20.
[153] S. Hecker, R. K. Reddy, T. Glinka, O. Rodny, (Rempex pharmaceuticals, Inc), *WO 2018/005662A1*, **2018**.
[154] R. Tsivkoski, M. Totrov, O. Lomovskaya, *Antimicrob. Agents Chemother.* **2020**, *64*, e00130-20.
[155] K. Nelson, D. Rubio-Aparicio, D. Sun, M. Dudley, O. Lomovskaya, *Antimicrob. Agents Chemother.* **2020**, *64*, e00757-20.
[156] E. A. Meyer, R. K. Castellano, F. Diederich, *Angew. Chem., Int. Ed.* **2003**, *42*, 1210.
[157] J. C. Gordon, J. B. Myers, T. Folta, V. Shoja, L. S. Heath, A. Onufriev, *Nucleic Acids Res.* **2005**, *33*, W368.
[158] http://biophysics.cs.vt.edu/H++ (acessed: November 2020).
[159] M. B. Peters, Y. Yang, B. Wang, L. Füsti-Molnár, M. N. Weaver, K. M. Merz, *J. Chem. Theory Comput.* **2010**, *6*, 2935.
[160] D. A. Case, D. S. Cerutti, T. E. Cheatham, III, T. A. Darden, R. E. Duke, T. J. Giese, H. Gohlke, A. W. Goetz, D. Greene, N. Homeyer, S. Izadi, A. Kovalenko, T. S. Lee, S. LeGrand, P. Li, C. Lin, J. Liu, T. Luchko, R. Luo, D. Mermelstein, K. M. Merz, G. Monard, H. Nguyen, I. Omelyan, A. Onufriev, F. Pan, R. Qi, D. R. Roe, A. Roitberg, C. Sagui, C. L. Simmerling, W. M. Botello-Smith, J. Swails, R. C. Walker, J. Wang, R. M. Wolf, X. Wu, L. Xiao, D. M. York, P. A. Kollman, AMBER 2017, University of California, San Francisco **2017**.
[161] Building bonded model with MCPB: https://ambermd.org/tutorials/advanced/tutorial20/mcpb.php (accessed: November **2020**).
[162] J. M. Seminario, *Int. J. Quantum Chem.* **1996**, *30*, 1271.
[163] W. D. Cornell, P. Cieplak, C. I. Bayly, I. R. Gould, K. M. Merz, Jr., D. M. Ferguson, D. C. Spellmeyer, T. Fox, J. W. Caldwell, P. A. Kollman, *J. Am. Chem. Soc.* **1995**, *117*, 5179.
[164] J. A. Maier, C. Martinez, K. Kasavajhala, L. Wickstrom, K. E. Hauser, C. Simmerling, *J. Chem. Theory Comput.* **2015**, *11*, 3696.
[165] A. W. Goetz, M. J. Williamson, D. Xu, D. Poole, S. Le Grand, R. C. Walker, *J. Chem. Theory Comput.* **2012**, *8*, 1542.
[166] R. Salomon-Ferrer, A. W. Goetz, D. Poole, S. Le Grand, R. C. Walker, *J. Chem. Theory Comput.* **2013**, *9*, 3878.
[167] S. Le Grand, A. W. Goetz, R. C. Walker, *Comput. Phys. Commun.* **2013**, *184*, 374.
[168] T. A. Darden, D. York, L. G. Pedersen, *J. Chem. Phys.* **1993**, *98*, 10089.
[169] J.-P. Ryckaert, G. Ciccotti, H. J. C. Berendsen, *J. Comput. Phys.* **1977**, *23*, 327.
[170] W. L. DeLano, *The PyMOL Molecular Graphics System*, DeLano Scientific LLC, Palo Alto, CA, USA **2008**. http://www.pymol.org.
[171] E. F. Pettersen, T. D. Goddard, C. C. Huang, G. S. Couch, D. M. Greenblatt, E. C. Meng, T. E. Ferrin, *J. Comput. Chem.* **2004**, *25*, 1605.
[172] D. R. Roe, T. E. Cheatham, *J. Chem. Theory Comput.* **2013**, *9*, 3084.
[173] AMBER 2015 London Workshop. Introduction to Principal Component Analysis: http://www.amber.utah.edu/AMBER-workshop/London-2015/pca/ (accessed: November **2020**).

Emilio Lence obtained his Ph.D. at the University of Santiago de Compostela (USC, Spain) in 2009. He did a predoctoral stay in the University of Cambridge (UK) with Professor Abell. After concluding his doctoral thesis, he joined the Department of Chemistry at the University of Bristol (UK) as a Xunta de Galicia postdoctoral fellow in Professor Mulholland's group. In 2015 he returned to the USC as a research associate, focusing his research on using computational tools to understand enzyme recognition and mechanistic processes with potential applications for the discovery of novel antibiotics and β-lactamase inhibitors.

Concepción González-Bello obtained her Ph.D. at the University of Santiago de Compostela (USC, Spain) in 1994. She did predoctoral stays at the University of Ghent (Belgium) with Professor Vandewalle and at the Scripps Research Institute (USA) with Professor Nicolaou. In 1994 she joined the University of Cambridge (UK) as a postdoc in Professor Abell's group. In 1996 she joined the USC as an assistant professor and was promoted to associate professor in 2003. Since 2011 she has been group leader at the CiQUS. Her main research interest is the structure-based design of novel antibiotics and β-lactamase inhibitors in the fight against superbugs.